uOttawa

L'Université canadienne
Canada's university

FACULTÉ DES ÉTUDES SUPÉRIEURES ET POSTOCTORALES

uOttawa

L'Université canadienne
Canada's university

FACULTY OF GRADUATE AND POSDOCTORAL STUDIES

Ramiel Nassara
AUTEUR DE LA THÈSE / AUTHOR OF THESIS

M.A.Sc. (Chemical Engineering)
GRADE / DEGREE

Department of Chemical Engineering
FACULTÉ, ÉCOLE, DÉPARTEMENT / FACULTY, SCHOOL, DEPARTMENT

Absorption Separation of Ethylene / Ethane
TITRE DE LA THÈSE / TITLE OF THESIS

Dr. F. Handan Tezel
DIRECTEUR (DIRECTRICE) DE LA THÈSE / THESIS SUPERVISOR

CO-DIRECTEUR (CO-DIRECTRICE) DE LA THÈSE / THESIS CO-SUPERVISOR

EXAMINATEURS (EXAMINATRICES) DE LA THÈSE / THESIS EXAMINERS

Dr. Jules Thibault

Dr. Mikhail Sorin

Dr. Poupak Mehrani

Gary W. Slater
Le Doyen de la Faculté des études supérieures et postdoctorales / Dean of the Faculty of Graduate and Postdoctoral Studies

Adsorption Separation of Ethylene/Ethane

By

Ramiel Nassara

A Thesis submitted in partial fulfillment
of the requirement for the degree of

M.A.Sc. in Chemical Engineering

in the

DEPARTMENT OF CHEMICAL ENGINEERING
UNIVERSITY OF OTTAWA

Ottawa, Canada August 20th, 2008

Research Director

Candidate

Your file Votre référence
ISBN: 978-0-494-48497-5
Our file Notre référence
ISBN: 978-0-494-48497-5

ABSTRACT

To offset rising energy costs, it is becoming a necessity to lower energy usage within industrial processes. Such can be said for the separation of olefin/paraffin mixtures. An example of such a mixture is ethylene/ethane. This highly energy intensive industrial separation employs cryogenic distillation to achieve a high purity product. Subsequently, the energy cost to run such a system is extremely high. Hybrid scenarios have been explored, with adsorption being a potential candidate. This work studied the potential of three adsorbents for the separation of ethylene/ethane: $AgNO_3/SiO_2$, $CuCl/SiO_2$, and CECA 13X. $AgNO_3/SiO_2$ and $CuCl/SiO_2$ were both prepared in the laboratory. Pure component constant volume experiments were conducted, along with binary mixture predictions for all three adsorbents at 3 different temperatures. The expected working capacities were also calculated for the three adsorbents. Finally, an economic analysis, without taking competitive adsorption in to factor, was conducted to give a rough idea of how much a potential PSA system would cost using the three adsorbents individually. $CuCl/SiO_2$ yielded the most favorable results of the three adsorbents, but more studies were determined necessary on the optimization of the preparation of the adsorbent. $AgNO_3/SiO_2$ was not completely ruled out, however. Both the adsorbents showed characteristics for a potential use within industry. CECA 13X was not considered a viable candidate for such a separation.

RÉSUMÉ

Pour compenser la croissance des coûts en énergie, il est nécessaire de diminuer la demande énergétique des procédés industriels. C'est le cas de la séparation des mélanges d'oléfines et de paraffines. Ce procédé industriel est très énergivore et requiert l'emploi d'une colonne de distillation cryogénique afin d'obtenir la pureté désirée. Des scénarios hybrides de séparation ont été étudiés et en particulier l'utilisation d'un procédé d'adsorption. Cette étude s'est intéressée à l'utilisation de trois adsorbants pour la séparation de l'éthylène et de l'éthane : $AgNO_3/SiO_2$, $CuCl/SiO_2$, and CECA 13X. Le $AgNO_3/SiO_2$ et le $CuCl/SiO_2$ ont été préparés en laboratoire. Les isothermes pour ces trois adsorbants ont été déterminées pour les composés purs et pour des mélanges binaires à trois différentes températures. Les capacités utiles des trois adsorbants ont été calculées. Finalement, une étude économique sans toutefois prendre en compte la compétitivité d'adsorption a été menée pour estimer les coûts pour un système d'adsorption cyclique par changement de pression et ce pour les trois adsorbants. L'utilisation du $CuCl/SiO_2$ semble être l'option la plus économique parmi les trois adsorbants mais une étude plus approfondie est nécessaire pour l'optimisation de sa synthèse. L'utilisation du $AgNO_3/SiO_2$ n'est toutefois pas écartée pour l'instant. Les deux adsorbants possèdent des caractéristiques qui les rendent aptes pour leur utilisation en industrie. Le CECA 13X n'est pas considéré un adsorbant acceptable pour une cette séparation.

1. ACKNOWLEDGEMENTS

I would like to thank Dr. Handan F. Tezel for her insight and help with this study. I would also like to thank Vinay Mulgundmath and the S.M.A.R.T. lab for my training on the constant volume system and further mentoring. Special thanks go to Gerard Nina, Franco Ziroldo, and Louis Germain Tremblay for their technical support with the constant volume system as well. Thank you goes to the University of Ottawa Chemical Engineering Department for a wonderful experience during my time there. Last but not least, I would like to thank my family for their support during my time at the University of Ottawa. Without their support, none of this would have been possible.

2. INTRODUCTION

The separation of olefin/paraffin is a section within the petroleum industry of great importance. This separation is also among the most costly within the industry. Cryogenic distillation is the process used to separate olefin/paraffin mixtures, using their sub-zero boiling points to remove one from the other. Cryogenic distillation has been employed for over 60 years for such separations (Padin & Yang, 2000). Cryogenic distillation is highly energy intensive and usually accounts for 25-50% of total energy costs for a plant (Ng et al., 2005). A department of energy report in the US estimated that 0.12 Quads (127×10^{12} kJ) is used for olefin/paraffin separations on an annual basis (Humphrey et al., 1991).

Olefins (or alkenes) represent a group of hydrocarbons with the general formula C_nH_{2n}, where n represents the number of carbon atoms. Paraffin's (or alkanes) are another group of hydrocarbons with the general formula C_nH_{2n+2} (Speight, 1991). These two groups have very similar molecular formulas, which explain their close relative volatilities (Padin & Yang, 2000). This similarity in relative volatilities yields a very difficult separation scenario. Molecular differences between olefin/paraffin mixtures have been further explored to more efficiently separate these two species. For example, molecular size and bond type could be exploited to separate ethylene from ethane.

The aforementioned molecular differences are used in this work by exploring adsorption as the separation process. Three adsorbents are experimented with using a constant volume system, in hopes that at least one of them will reveal some potential to help in the reduction of the energy costs associated with this separation. $AgNO_3/SiO_2$, $CuCl/SiO_2$, and CECA 13X are compared experimentally as potential adsorbents to aid

the separation of ethylene from ethane. Since ethylene has a double bond, and is the smaller of the two molecules, it should be adsorbed with higher capacity within the metal cation impregnated silica gel and zeolite.

$AgNO_3/SiO_2$ has been used in previous work for similar applications. As such, the constant volume system experimental values of $AgNO_3/SiO_2$ for ethylene obtained are compared to previous work conducting similar experimentation to test for consistency. Two other adsorbents in $CuCl/SiO_2$ and CECA 13X are studied as well and compared to $AgNO_3/SiO_2$. The constant volume experimental data in this study explores higher pressures as well as sub zero adsorption temperatures. These higher pressures and lower temperatures give a broader understanding of the capabilities of the adsorbents used in this work, as industrial practices would yield both conditions. All experiments were performed using pure component gases. Regeneration experiments were also conducted using the constant volume system. These experiments tested the reusability of $AgNO_3/SiO_2$, an already established potential candidate for olefin/paraffin separations. Preliminary $CuCl/SiO_2$ preparation optimization was experimented on as well in this study.

Although only pure component data was collected, binary behaviour was predicted using the ideal adsorbed solution theory. The expected working capacity for both ethylene and ethane were calculated based on the different temperatures used in the constant volume experiments as well. Finally, the experimental values from all three adsorbents are used to conduct simple economic analysis to compare the operating cost of the three adsorbent beds.

3. LITERATURE SURVEY

The following section contains the topics used to further support the experimental design of this work. The section begins with an introduction to the adsorbate studied, followed by theoretical background of adsorption and the adsorbents used in this work. The models used in conjunction with the experimental values are also introduced.

3.1 Ethylene/Ethane

One of the most important olefin/paraffin separations is ethylene-ethane. Ethylene is used mostly as an intermediate for the production of plastics. Ethylene can be polymerized to directly make polyethylene. Polyethylene is the world's most widely used plastic. Plastic bags, water bottles, etc. are made using polyethylene. Ethylene can be used with benzene to create ethyl benzene, which is used in the production of polystyrene. Polystyrene is also another widely used plastic. Other minor uses of ethylene include anaesthetics, crop ripening, and welding (IPCS, 2005). The global demand for ethylene in 2005 was in excess of 100 000 000 tons. Ethane on the other hand, has its main use in the production for ethylene via steam cracking. Ethane is diluted with steam and is then briefly heated to a very high temperature of 900°C or higher. Ethane is chosen because it is highly selective to ethylene when broken down, whereas heavier hydrocarbons tend to yield greater mixtures of propylene and butadiene (Ren et al., 2006).

Table 1: Ethylene/Ethane Properties

Property \ Component	Ethylene	Ethane
Molecular Weight	28.05 g/mol	30.07 g/mol
Boiling Point (At 1 atm)	-104 °C	-88.55 °C
Carbon Bond	Double	Single
Kinetic Diameter	3.9 Å	4.75 Å

Some properties of ethylene and ethane are given in Table 1. Normal boiling point of ethylene and ethane are -103.7 °C, and -88.6 °C, respectively. The difference in these two temperatures automatically makes this separation as a candidate for cryogenic distillation. However, this process is very energy intensive. Energy costs being on the rise, an alternative route is highly desirable to save on operating costs. The capital cost alone for a world-class ethylene processing unit is over $500 000 000. The major part of this cost is the olefin/paraffin separation portion (Eldridge, 1993). It leaves the challenge of reducing energy costs to compensate for such large capital costs. It is also important to consider that the purity of the product already established with cryogenic distillation is maintained with whichever alternative replaces it. Table 1 lists physical properties of both ethylene and ethane. Inspection of this table shows that there are molecular differences that could be potentially exploited for separation purposes. The kinetic diameters listed in this table yield a promise to possibly use the steric effect to separate these two substances by exploiting their size differences. Furthermore, the more reactive double bond in ethylene can be utilized for separation purposes, as well.

3.2 Adsorption Process Considered

Alternatives such as absorption, adsorption, and membrane separations have been studied in the literature (Eldridge, 1993). Of these choices, a promising route would be the use of π-complexation via adsorption. Adsorption has the potential of being a more

energy efficient alternative for separation than the already established cryogenic distillation systems in place. The energy efficiency lies in the potential to separate the two components by using their molecular differences, rather than their thermodynamic properties. Cryogenic distillation uses the components boiling point differences and as such, is required to maintain sub-zero temperatures at high pressures, which is quite energy intensive. Adsorption would allow these high pressure mixtures to be separated without the necessity of high energy costs, but by separating based on the size difference. Ethylene is the smaller of the two adsorbate, so it would be assumed based on steric effects alone, that it would be adsorbed at a higher rate. Pressurization costs of the adsorption units would be nullified based on the already high pressure feeds coming in to the adsorption column. Desorption would be as simple as lowering the pressure of your product stream to recover the product captured during adsorption. π-complexation offers a potential route of adsorption that would successfully separate olefins from paraffin's.

To understand π-complexation however, adsorption in general must be first introduced. Adsorption uses porous solids to adsorb large volumes of gas/vapour/liquids. Desorption is the release of the gas/vapour/liquid. Adsorption can be classified in to two types: physical and chemical. Physical adsorption is caused mostly by van der Waals and electrostatic forces between adsorbate molecules and the adsorbent surface. A high surface area is preferable for allowing a high adsorption capacity. A distinguishing characteristic of physical adsorption is that since the bonds are weaker than that of chemical adsorption, the adsorbate may be evacuated from the adsorbent at the same temperature by using a pressure drop in the column to release the molecules. Chemical adsorption (or chemisorptions) involves much stronger forces than physical adsorption.

To evacuate an adsorbate after chemisorptions, a temperature and/or pressure change may be necessary. As the temperature increases, the capacity of the adsorbent decreases in both, physical and chemical, adsorption (Suzuki, 1990). Table 2 shows distinguishing characteristics between physical and chemical adsorption.

Table 2: Physical/Chemical Adsorption Characteristics (Ruthven, 1984)

Parameter	Physical Adsorption	Chemical Adsorption
Desorption	By reduced pressure or increased temperature. Physical properties of adsorbent the same.	High temperatures required to break strong bonds. Adsorbent physical properties may vary.
Specificity	Non-specific.	Very specific.
Dissociation & Electron Transfer	No dissociation and no electron transfer.	Both dissociation and electron transfer.
Heat of Adsorption (kJ/mol)	Low heat of adsorption (20-40, Exothermic).	High heat of adsorption (>80, Exothermic/Endothermic)
Nature of Phase Adsorbed	Monolayer/Multilayer (Depending on conditions).	Monolayer only.

3.3 π-complexation

π-complexation is a sub-group of chemical complexation where the mixture is brought into contact with a second phase containing a complexing agent (King, 1987). The mixture in this case is ethylene-ethane and the complexing agent is the adsorbent of choice. The bonds formed in chemical complexation are much stronger than those of Van Der Waals forces alone. This allows for high selectivity achievement, along with a high capacity for the component to be bound. Fortunately, it is possible to break the aforementioned bonds by simply raising the temperature and decreasing the pressure of the system (Padin & Yang., 2000). π-complexation pertains to the main group of transition metals. This includes from Sc to Cu, Y to Ag, and La to Au (Rege et al.,

1998). The electrons transfer from the fully occupied 4d orbital of the transition metal to the 2p* (anti-bonding p) orbital of the adsorbate molecule (Chen et al, 1996). Figure 1 displays an example of π-complexation in which Ag bonds with ethylene.

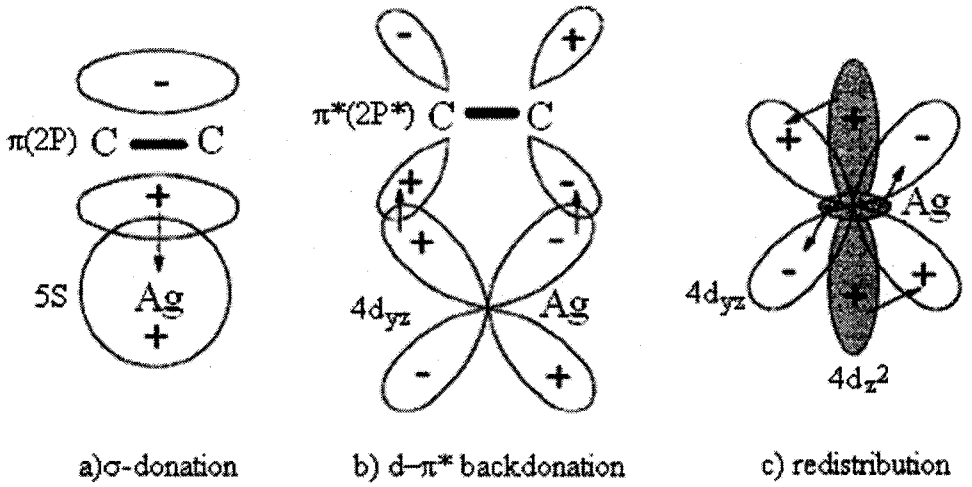

Figure 1: C_2H_4-Ag exchanges via π-complexation (Chen et al, 1996).

Figure 2 displays the Figure 1 process from a complete molecule viewpoint to further emphasize the bonding process.

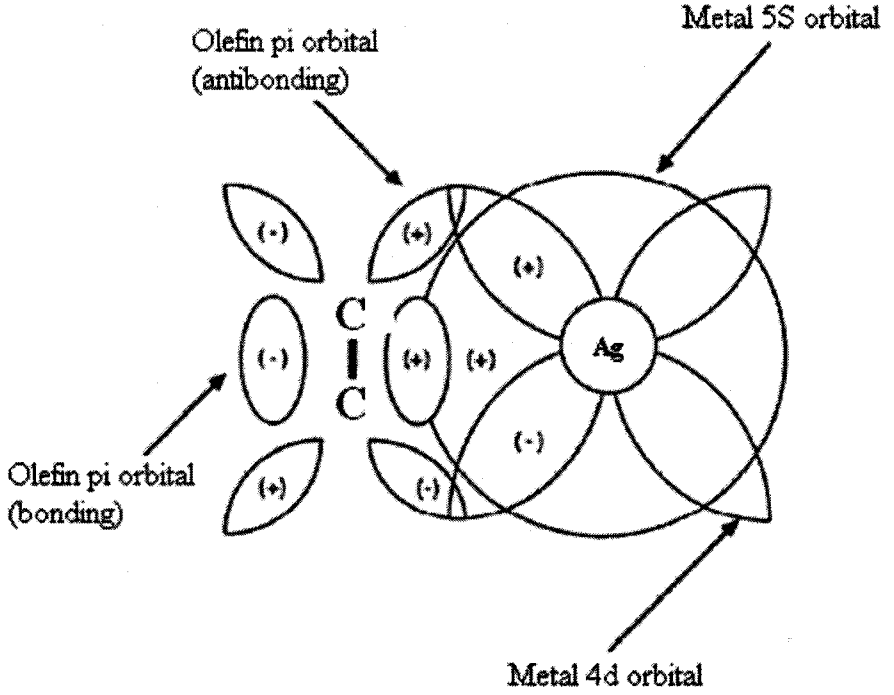

Figure 2: C_2H_4-Ag complete molecule π-complexation (Eldridge, 1993).

3.4 Adsorption/Desorption Scenarios

Depending on the regeneration conditions of the adsorbent, the adsorption process may vary. If the adsorption is of physical nature, then pressure swing adsorption (PSA) can be used. PSA systems utilize differences in adsorbent capacities under different pressure conditions. There is no heat added to the system, so the temperature is to remain constant throughout the process. There is however an expected increase in temperature within the unit however, due to adsorption being an exothermic reaction. This phenomena is known as heat of adsorption and is further discussed in §4.6. Adsorption within the adsorbent bed is performed at an elevated pressure and for desorption, a lower pressure is chosen to separate the adsorbent from the adsorbed chemical. In this scheme, desorption pressure is constant, while the adsorption pressure is varied accordingly.

A similar process to PSA is known as Vacuum Swing Adsorption (VSA). This process involves adsorption occurring at atmospheric pressure and desorption is then achieved under vacuum conditions. The utilisation of capacity differences at different pressures is similar in both a PSA and VSA. The pressure regions utilized are what make these two systems different though. The adsorption unit temperature is constant when using VSA as well. A VSA system varies the desorption pressure, while keeping the adsorption pressure constant.

The third and final adsorption process is known as Temperature Swing Adsorption (TSA) and is best utilized under chemisorptions conditions. TSA utilizes differences in capacity based on temperature to separate components with stronger bonds. The pressure is kept constant in this process. A lower temperature is used for adsorption, while to desorb a higher temperature is used. This is based on the fact that when

temperature increases an adsorbents capacity will decrease, thus releasing the captured chemical.

These processes can be combined in some cases if one factor change is not enough to effectively remove the adsorbate from the adsorbent. Such cases include TPSA and TVSA. TPSA stands for Temperature Pressure Swing Adsorption and this process involves both a decrease in pressure and increase in temperature to allow for optimal adsorbate recovery during desorption of the columns. In the case of Temperature Vacuum Swing Adsorption, the combination of both a decrease below 1 atm in pressure and an elevated temperature would be used for desorption. Figure 3 is a simple schematic diagram of an adsorption system that can represent all the above processes. In this figure, numbers 1 and 2 represent columns that are packed with the adsorbent that is going to separate a mixture of components A and B.

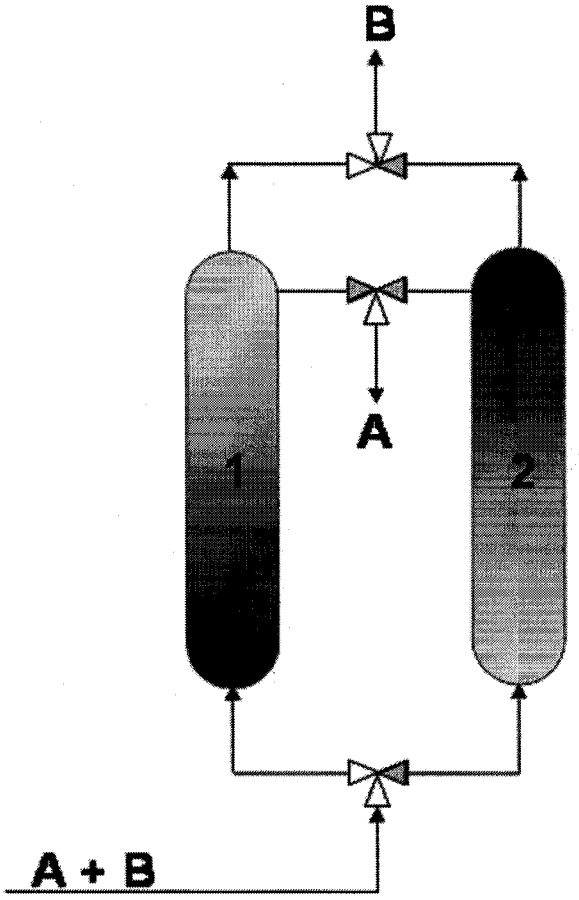

Figure 3: Schematic Diagram of PSA/VSA/TSA/TPSA/TVSA

In all three cases, the mixture would enter column 1, while the valve to column 2 is closed. Within the column, there is an adsorbent packed bed. The mixture A+B enters the column and species A is adsorbed, while species B exits through the top. The valves are closed on the left side of the diagram at the top and bottom, while the middle one is now opened. The right side valves are now opened as well, leaving the middle one on the right closed. Now desorption occurs in column 1, while a new mixture of A+B is sent in to column 2 to be adsorbed. This process is a continuous cycle with both desorption and adsorption occurring simultaneously.

The differences between the processes lie in the desorption step of each process. In PSA, column 1 would have a pressure drop below that of the adsorption pressure. 1

atm is the conventional choice for desorption, but can vary from process to process. For VSA, desorption pressure would be set below 1 atm by vacuum. For TSA, the temperature would be elevated above the adsorption temperature to desorb the bed. For TPSA, the temperature would be elevated and the pressure would be decreased below the temperature and pressure of adsorption to recover A during desorption. Similarly, the temperature would be decreased and the pressure decreased for TVSA processes. As in VSA and PSA, the differing factor is the adsorption pressure in TPSA and TVSA. In TPSA, the adsorption pressure is above 1 atm and for desorption it is lowered accordingly. In TVSA, the adsorption pressure is at 1 atm and is lowered below this value via vacuum. The combination of temperature elevation and pressure drop act as an effective process of recovery in both physical and chemical adsorption cases.

3.5 Choice of Adsorbents

In choosing an adsorbent, there are important characteristics to use as deciding factors. These include the separation factor, adsorption capacity, ease of regeneration, reactivity toward the adsorbate, and last but especially not least, cost (Choudary & Mayadevi, 1993). Since adsorption is an exothermic process, the heat of adsorption is essentially a measure of ease of regeneration. The higher the value, the more energy intensive desorption may be. A general range for heat of adsorption is 20 – 30 kJ/mol. Reactivity between the adsorbent and adsorbate would further lend to ease of regeneration. Since the adsorbent is temporary accommodation for the adsorbate, a strong reaction between the two could possibly alter the adsorbate and diminish the end product recovered in the process. Adsorption capacity is a straight forward measurement of how much adsorbate can be held within the adsorbent using an experimental set up

known as the constant volume system later discussed in this paper. Separation factor lends itself as another important characteristic to adsorbent choice for the simple fact that if the separation difference between the two species in the process is small, then obtaining a high purity end product tends to be increasingly difficult. Cost is a straight forward measure of adsorbent choice. If the adsorbent costs too much to use, then there is no real benefit to use it.

The capability of activated carbon for pure component ethane and ethylene systems was studied by Byoung et al. (2003). Temperatures ranging from 20 °C – 40 °C were studied at pressures as high as 18 atm. The results were not promising however. Both adsorbates were adsorbed at high capacities very similar to each other. Furthermore, the trend began to show signs of reaching saturation at above 6 atm. This peaking of the adsorbent is not ideal for separations because the difference between the adsorption capacity and desorption capacity may be very minimal.

Wu et al. (1997) experimented with Ag^+ ion-exchanged resins for ethylene/ethane adsorption applications with positive results. . The experiments were completed at 25 °C and up to approximately 1 atm. Ag^+ was exchanged most successfully on to Amberlyst 35. The results of the ion-exchanged resin versus that of the typical resin were quite promising. The difference in capacity for ethylene and ethane was much larger when Ag^+ was exchanged on to the substrate. However, due to the low pressures experimented at in this study; it is hard to conclude that the previously mentioned adsorbent is the most appropriate candidate for ethane/ethylene separations. This study was an excellent example of the positive results of π-complexation on ethane/ethylene separation. It also emphasizes the potential of using Ag^+ effectively for separation of ethane/ethylene.

In previous studies, $AgNO_3/SiO_2$ was determined to have high potential for olefin/paraffin separations. Likewise, it is known that CuCl has a higher affinity for olefins than $AgNO_3$. It has been proposed that if impregnated in a highly porous substrate, it could also yield high potential for olefin/paraffin separations. Zeolites have previously been attempted for olefin/paraffin separations, but have not yielded as successful results as the two adsorbents previously mentioned (Rege et. al, 1998). CECA 13X was used to further study its potential uses in this field.

The $AgNO_3/SiO_2$ was successfully synthesized using incipient wet impregnation. This technique is standard for catalyst preparation in industry (Padin & Yang, 2000). $CuCl/SiO_2$ was prepared using Monolayer Thermal Dispersion. Multiple samples were prepared based on CuCl to SiO_2 ratios in the mixture. The best performing ratio, in terms of capacity for ethylene, was then used to perform a study on the effects of the sample prepared based on temperature differences. CECA 13X was obtained through an industry source.

3.6 $AgNO_3/SiO_2$ Studies

Previous research has been established in literature on types of adsorbents for olefin/paraffin adsorption. In one such study, six potential adsorbents were compared in the adsorption of ethane, methane, carbon dioxide, and ethylene. The adsorbents were H-ZSM-5, Na-ZSM-5, H-ZSM-8, Na-ZSM-8, Silicalite, and ALPO-5 from 303 – 473 K. It was determined in this study that ALPO-5 showed the lowest heat of adsorption for ethane and ethylene. It was further determined that ZSM-5 and ZSM-8 type adsorbents are reactive towards ethylene and ethane, making them unsuitable for separating mixtures of this kind. Silicalite had comparable results to that of ALPO-5, but due to the lower

heat of adsorption exhibited by ALPO-5, it was determined that Silicalite was not as promising (Choudary & Mayadevi, 1993). Further investigation of ALPO-5 showed that it was not readily available commercially or easily produced on a laboratory scale level. This lends to the idea that the production of this adsorbent, although promising to the application, may incur too much of a cost to be viable.

It is necessary to impregnate the SiO_2 with $AgNO_3$ to create the adsorbent because in previous work, it was shown that simply using SiO_2 as the adsorbent would not yield uptake values as high as the impregnated SiO_2 (Padin & Yang, 2000). The selectivity of SiO_2 alone was found to be 1.5, while the selectivity for ethylene in the $AgNO_3/SiO_2$ was 4. In this same work, comparisons of three high surface area substrates were compared as well. The three surfaces were SiO_2, MCM-41 mesoporous zeolite, and γ-Al_2O_3 (Padin & Yang, 2000). It was determined that when impregnated by $AgNO_3$, SiO_2 yielded the best results.

Wet impregnation was used because it was determined in the aforementioned work (Padin & Yang, 2000) that it was a more effective method of impregnation than for instance, thermal monolayer dispersion. Wet impregnation allows for a more even dispersion of the salt, with less pore blockage than the aforementioned monolayer dispersion. Wet impregnation involves making a solution of the salt to be dispersed during impregnation. The salt must be very soluble within the solvent of choice. While choosing a solvent, the affinity of the substrate for the solvent must also be considered. This allows proper wetting of the substrate surface, allowing even dispersion of the salt.

In another study by this group, $AlPO_4$-14 and $AgNO_3/SiO_2$ were compared for the separation of propane/propylene, a heavier mixture, but similar in molecular differences

to ethylene/ethane. This comparison was performed using a computer simulated PSA system using a proven mathematical model. The performance of $AgNO_3/SiO_2$ was found to be better than zeolite 4A based on much higher selectivity for C_3H_6 and faster kinetics. It was determined that $AlPO_4$-14 had a slightly better recovery than $AgNO_3/SiO_2$, but with the consequence of lower capacity. In this case the $AgNO_3/SiO_2$ once again was the clear choice for adsorption of propylene/propane (Rege et al., 2002).

In another work by a different group conducted for ethylene adsorption, the uptake of zeolite 4A was determined to have a similar capacity for ethylene as that of $AgNO_3/SiO_2$. However, the difference was in the capacity for ethane uptake. $AgNO_3/SiO_2$ held a lower capacity for ethane at similar conditions than zeolite 4A (Rege et al., 1998). Furthermore, the product recovery via desorption was lower for zeolite 4A than that of $AgNO_3/SiO_2$. Carbon Molecular Sieve and Ag^+ resin were used in adsorption also in the previous study. It was determined that $AgNO_3/SiO_2$ shared a similar selectivity to that of Ag^+ resin for ethylene, but Ag^+ did not share the same capacity for ethylene as $AgNO_3/SiO_2$. The Ag^+ resin had a lower capacity for ethylene than the $AgNO_3/SiO_2$. It was also determined that the Carbon Molecular Sieve adsorbent had a high adsorption capacity, but product recovery was much more difficult (Rege et al., 1998). All of the adsorbents had a positive feature in ethylene/ethane separation, however, only $AgNO_3/SiO_2$ outperformed in all aspects including capacity, selectivity, and recovery. Therefore, it was chosen to be studied further in this study.

3.7 $CuCl/SiO_2$ Studies

$CuCl/SiO_2$ was chosen as the second adsorbent because copper cations are known to have a higher affinity for olefins than silver do. For example, Blas et al. (1998) found

that by the addition of CuCl on to a high capacity substrate such as γ-Al_2O_3, the capacity for ethylene was increased appreciably. It was mentioned in other literature that by impregnating a high surface area compound with copper cations, the performance of this adsorbent theoretically should be better than that of $AgNO_3/SiO_2$ (Yang, 2003). An example of using CuCl impregnated substrates is found in literature in which the substrate is actually pillared clay. This process was considered unsuccessful, however. The capacity for the selected pressure regions was considered quite competitive, but the data revealed an unfavourable logarithmic shape. The data strayed from linearity, which is important for this process, as it allows for a larger difference in adsorption and desorption capacities (Cheng & Yang, 1995).

The only problem with impregnating SiO_2 with CuCl is that there is no solvent that can be used that CuCl will dissolve in that silica gel has a high affinity for and won't dissolve in itself. Weak acids can easily dissolve CuCl, but will simultaneously dissolve SiO_2. Another option is to use thermal dispersion rather than wet impregnation and cause a fusion between the two substances. Although proven not to be as effective as wet impregnation in other adsorbent preparations as in $AgNO_3/SiO_2$, it is a valid choice in this case. To perform thermal impregnation, a salt is evenly dispersed across a substrate (in our case CuCl and SiO_2) at a predetermined mass ratio. The mixture is then heated to what is referred to as the Tammann temperature. The Tammann temperature is 30 – 70% of the absolute melting point of the salt. Normally, one could use 50% as a reasonable starting point. The salt molecules are then disrupted and begin to fuse to the substrate, hopefully not blocking the pores. Unfortunately, the pores are usually more blocked than

when using wet impregnation, which is why wet impregnation is preferred (Padin & Yang, 2000).

3.8 CECA 13X Studies

As previously discussed, zeolites have yielded great capacity results with the limitations being in the small capacity difference between the olefin and the paraffin. CECA 13X will be explored to investigate its potential uses in this field. Previous work successfully accomplished with this adsorbent has included methane, CO_2, and nitrogen for land fill gas applications within the lab group.

3.9 Modelling Isotherms

Three models are chosen to express the experimental adsorption isotherm data: Langmuir, Tóth, and Temperature Dependent Tóth (TD-Tóth). The Langmuir theory was the first theoretical treatment of adsorption on solid surfaces. When attractive interactions between adsorbed molecules are neglected, it describes localized, monolayer adsorption on homogeneous adsorbent (Tóth, 2002). The Langmuir equation is given in equation 1

$$q = \frac{q_s bP}{1 + bP} \qquad [1]$$

The empirical Tóth equation is an extension of the Langmuir equation. With the addition of the Tóth parameter, t, it is proposed to fit data more accurately. Equation 2 shows the empirical Tóth equation.

$$q = \frac{q_s bP}{\left[1 + (bP)^t\right]^{1/t}} \qquad [2]$$

A further extension of the Langmuir and Tóth equations is the Temperature Dependent Tóth equation. The Tóth equation is still employed; however the difference

lies in the parameter calculation. The Tóth equation fits the experimental data directly to the three main parameters in the equation. The TD-Tóth involves the calculation of the same three parameters; n_s, b, and t as a function of temperature. Equations 3 – 5 show these parameters.

$$q_s = q_{s,o} e^{\left[\chi\left(1-\frac{T}{T_o}\right)\right]} \quad [3]$$

$$t = t_o + \alpha\left(1-\frac{T_o}{T}\right) \quad [4]$$

$$b = b_o e^{\left[\frac{Q}{RT_o}\left(\frac{T_o}{T}-1\right)\right]} \quad [5]$$

All constants within the equations can be determined using experimental data and minimizing the weighted sum of squares residual within Microsoft Excel using Solver. For the Langmuir and Tóth isotherms, different temperatures had different parameters, whereas for the TD – Tóth Model, the experimental data for both temperatures were considered for the determination of the parameters. The advantage of the TD – Tóth is when these parameters are determined as a function of temperature; it leaves the possibility of both interpolation and extrapolation of the adsorption capacity values to the conditions that are not determined experimentally.

When fitting isotherm models to actual data, the precision of each model can be compared by using the sum of squared residual (SSR) values. The smaller the sum of these residuals, the more precise the model can be considered and thus, a more applicable model can be determined. Equation 8 defines the sum of squared residuals.

$$SSR = (s - \hat{s})^2 \quad [6]$$

3.10 Prediction of Binary Adsorption Behaviour

Equations [1] – [5] are all applicable to single component gas phase adsorption. An equation relating binary systems exists in the form of the Extended-Langmuir equation. The same assumptions are made in this extension of the Langmuir equation. Taking the predicted parameters from the pure system Langmuir equation for two different gases, one can predict the adsorption behaviour of a binary system consisting of these two gases. The Extended-Langmuir equation is given as:

$$q_i = \frac{q_{s,i} b_i P y_i}{1 + \sum_{j=1}^{2} b_j P y_i} \qquad [7]$$

Another method for predicting binary behaviour is the Ideal Adsorbed Solution Theory (IAST). This model assumes that the mixture behaves like an ideal solution, which means that all like and unlike molecules will interact in the same fashion. If the Langmuir model fits the experimental data well, the IAST forms the system of Equations 8, 9, 10 and 11:

$$q_1^{\infty} \ln(1 + B_1 P_1^o) = q_2^{\infty} \ln(1 + B_2 P_2^o) \qquad [8]$$

$$q_1^o = \frac{B_1 P_1^o}{1 + B_1 P_1^o} \qquad [9]$$

$$q_2^o = \frac{B_2 P_2^o}{1 + B_2 P_2^o} \qquad [10]$$

$$\frac{1}{q_t} = \frac{x_1}{q_1^o} + \frac{x_2}{q_2^o} \qquad [11]$$

Equation 8 – 11 can be used to ultimately calculate the competitive adsorption capacity for each component in the system. By using the Langmuir constants previously calculated during isotherm fits, one can solve Equation 8 through regression to find

values for P_1^o and P_2^o. Once these values are found, Equations 9 and 10 are used to calculate q_1^o and q_2^o. A total capacity, q_t, can be calculated from Equation 11 and thus using individual component mole fractions ranging from 0 to 1, the competitive adsorption capacities can be solved for each component in the system.

4. EXPERIMENTAL METHOD

4.1 Preparation of the $AgNO_3/SiO_2$ Adsorbent

The general method in which the adsorbent was made was taken from a previous study (Padin & Yang, 2000). As mentioned before, the salt must be very soluble within the solvent of choice. Choosing a solvent involves examining the affinity of the substrate for the solvent. Proper wetting of the substrate surface then applies, allowing even dispersion of the salt. In this work, water was chosen as the solvent. $AgNO_3$ is highly soluble in water and SiO_2 has a high affinity for water as well. The high affinity causes the water to be accepted within the porous material very easily. This meets the previously mentioned criteria.

Padin & Yang (2000) stated that a ratio of 0.32 g $AgNO_3$ to 1 g SiO_2 yields the best results for the adsorption of ethylene from the mixture. Therefore, the sample size of $AgNO_3$ and SiO_2 was chosen to be 16 g and 50 g, respectively. A 1.2 M solution of distilled water and $AgNO_3$ was thoroughly mixed. To create this solution using 16 g of $AgNO_3$, 78.5 mL of distilled water was needed. The solution was then mixed with 50 g of SiO_2. A Vulcan 3350 oven open to air was used to heat the sample to 105°C for 4 hours. This caused the water to evaporate and left $AgNO_3$ deposited in the pores of the SiO_2. The temperature was measured using a digital readout on the exterior of the oven.

Initially, $AgNO_3$ was a fine, white crystal and SiO_2 was a fine, white powder. After the water had evaporated from the mixture though, the impregnated SiO_2 exhibited a colour change to light beige. The finished product was a very fine, light beige powder. Figure 4 is a photograph of the finished product after transferring the product to a plastic container.

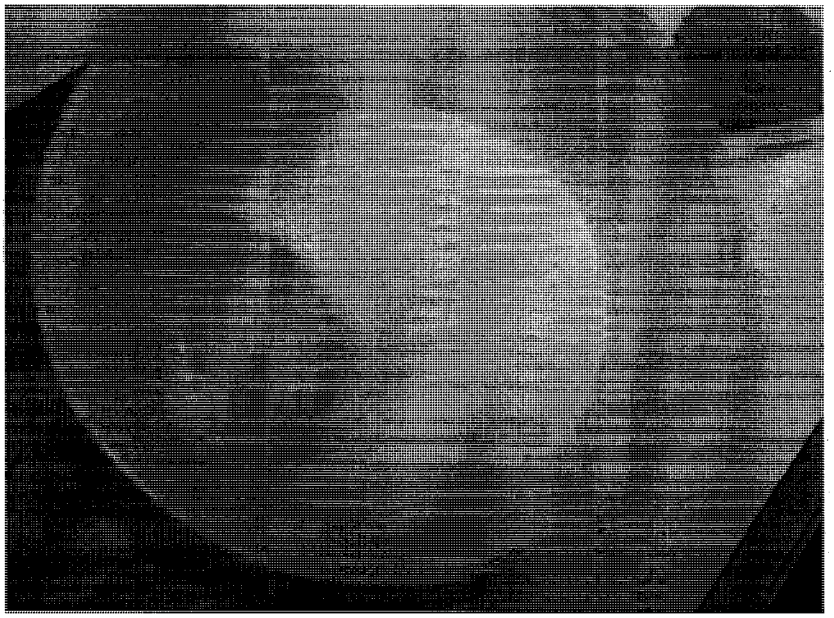

Figure 4: $AgNO_3/SiO_2$ Finished Product

4.2 Preparation of the $CuCl/SiO_2$ Adsorbent

Unfortunately, the wet impregnation technique could not be utilized for the impregnation of SiO_2 with CuCl because there was no solvent available that CuCl was soluble in and that SiO_2 accepted easily within its pores. For example, CuCl is highly soluble in acids, but at the same time, so is SiO_2. Mixing both these components in an acid would not yield the necessary results. This left the possibility of using monolayer thermal dispersion to disperse the salt across the SiO_2 pores. There was no literature found that had determined optimized conditions for this form of preparation of $CuCl/SiO_2$ as of yet. Initially, certain parameters needed to be chosen. The parameters were $CuCl/SiO_2$ mixture ratio, preparation temperature, and time. These specific variables would need to be optimized. For the purpose of this work however, our interest was simply to see if $CuCl/SiO_2$ could outperform $AgNO_3/SiO_2$ under similar experimental conditions. Table 3 lists the parameter combinations used to prepare the $CuCl/SiO_2$ samples in order of preparation.

Table 3: CuCl Preparation Parameters

CuCl/SiO_2 Ratio (g CuCl/g SiO_2)	Oven Temperature (°C)	Sample Time in Oven (h)
0.327	412	48
0.546	412	48
0.999	412	48
0.173	412	48
0.173	212	48
0.173	80	48

A final ratio of 0.000 g CuCl/ g SiO_2 was used as a comparison with the other samples to study whether or not there was an improvement in capacity of the SiO_2 after the thermal impregnation was performed. All these experiments were performed with C_2H_4 as the adsorbate at a temperature of 34°C.

4.3 CECA 13X Background

CECA Specialty Chemicals developed the 13X zeolite used in this study initially to be used in gas sweetening applications (CECA, 2008). As previously mentioned, zeolites have had high capacities for olefins and paraffin's, so it was proposed that CECA 13X be experimented with for ethylene/ethane applications to study its performance.

4.4 Collecting Experimental Data

A constant volume system was used to collect the pure component isotherm data. Figures 5 and 6 are photographs of the actual system used and an in-depth schematic diagram of the constant volume system, respectively.

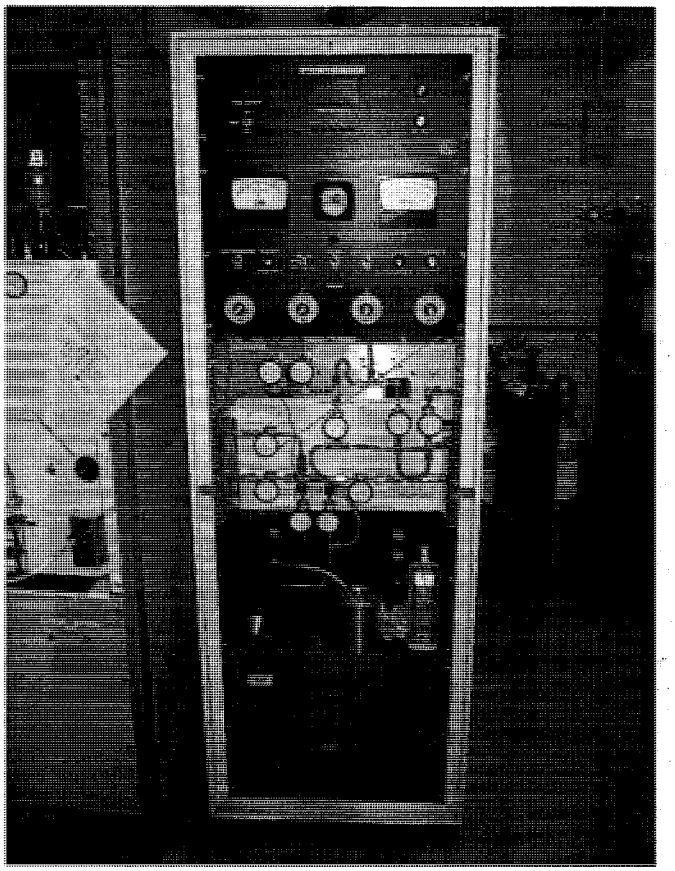

Figure 5: Photograph of the Constant Volume System

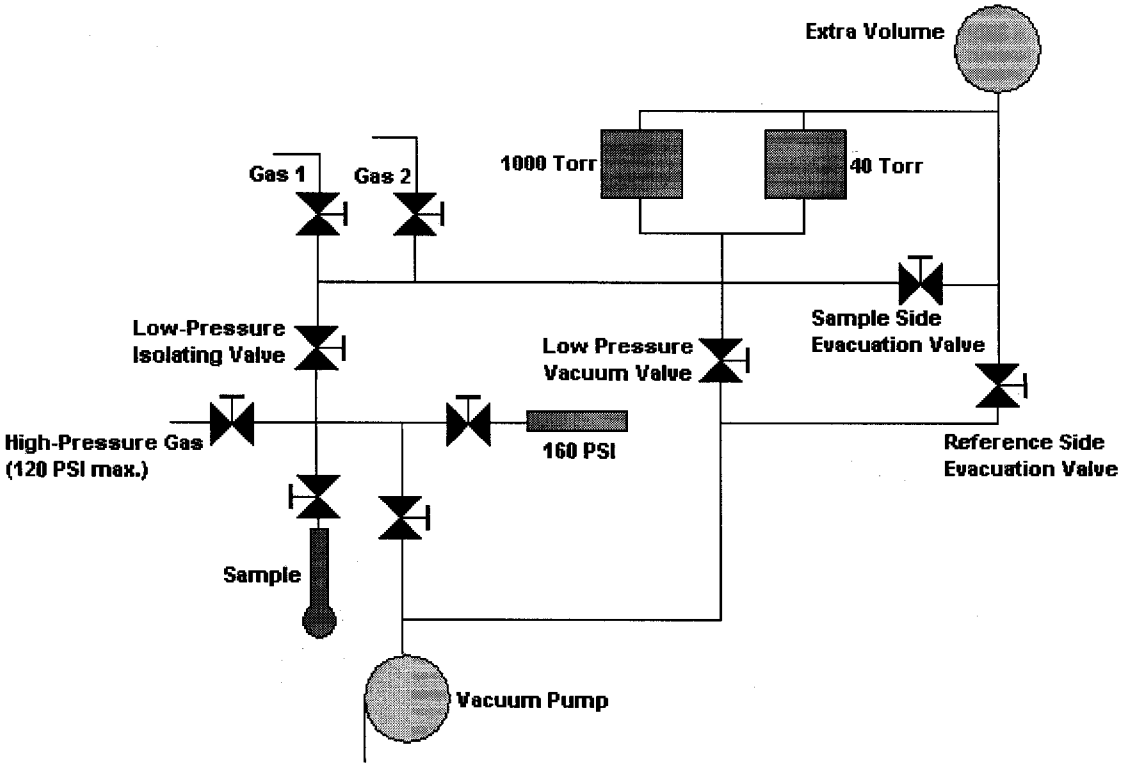

Figure 6: Schematic Diagram of the Constant Volume System

A sample of approximately 2 g was measured for the experiment and placed in the sample tube. Keeping as much air out of the tube as possible was important as to not overly contaminate the adsorbent before regeneration. The sample was regenerated at approximately 350 °C overnight (Padin et al., 2000). The total regeneration time was approximately 16 hours for each run performed. The regeneration was used to remove all possible contaminants in the system using helium as the regeneration gas, as well as the carrier gas. Once the regeneration was completed, the helium was used to measure the void volume within system. Heating the sample was possible using a heater attached to the constant volume unit. This was used for two purposes; regeneration of the sample and keeping the sample at a constant temperature for readings. For sub zero temperatures, the sample tube was placed within the confines of a thermos containing dry ice. The dry ice was monitored constantly and continuously refilled to replenish the sublimated dry ice. This allowed the sample temperature to remain constant. Two readings were taken per single data point. The first was a reading for the stabilized gas within the manifold, not including the sample tube. The sample tube was closed off for the initial point. Once the helium gas stabilized within the manifold, the sample valve was opened carefully, so as to not let any of the fine powder raise in to the manifold due to a quick pressure change.

The second pressure reading was when the gas was allowed in to the sample cylinder. Initially, there is a large pressure drop that indicates the extra volume being introduced within the sample cylinder and then there was a slower pressure change. This second, gradual change signified that adsorption was taking place. Manifold readings took less than a half hour to stabilize, while the second sample readings usually took

approximately twenty four hours. Eight to eleven data points consisting of a manifold reading and sample reading were taken in total per isotherm. In regards to the $CuCl/SiO_2$ parameter tests, only 3 to 4 points were taken across a broad pressure range to analyze the general differences between parameter changes. The first three to four points for $AgNO_3/SiO_2$ and CECA 13X were taken with the 0.75 atm pressure transducer, while the final five to seven were taken with the 11 atm transducer. For $CuCl/SiO_2$, only the first couple of points were taken with the 0.75 atm pressure transducer and the rest were taken with the 11 atm transducer. The constant volume system experiments are summarized in Table 4 in no particular order.

Table 4: Constant Volume Experimental Summary

Adsorbent	Adsorbate	Adsorption Temperatures (°C)		Regeneration Temperature (°C)	Purpose
		Experimental (This study, 2007)	Literature (Padin & Yang, 2000)		
$AgNO_3/SiO_2$	C_2H_4	-70, 34	70	350	Isotherm
$AgNO_3/SiO_2$	C_2H_6	-70, 34	70	350	Isotherm
$AgNO_3/SiO_2$	C_2H_4	34	-	350 200 25	Regeneration Test 1
$AgNO_3/SiO_2$	C_2H_4	35	-	350 25 25	Regeneration Test 2
$CuCl/SiO_2$	C_2H_4	-73, 34, 76	-	350	Isotherm
$CuCl/SiO_2$	C_2H_6	-73, 34, 76	-	350	Isotherm
CECA 13X	C_2H_4	-73, 34, 76	-	350	Isotherm
CECA 13X	C_2H_6	-73, 34, 76	-	350	Isotherm

It will be noted that the regeneration tests were two tests performed to further explore the possibility of $AgNO_3/SiO_2$ as the potential adsorbent of choice. The strong literature support of the adsorbent led to the exploration of how well it performed under different regeneration temperatures (Regeneration Test 1). The 2^{nd} regeneration test was used to explore how well the adsorbent worked after high pressure adsorption occurred followed by only vacuum regeneration. As noted in the 3^{rd} and 4^{th} lines of Table 4, all

regeneration tests were conducted using C_2H_4 at an adsorption temperature of 34 °C. Table 5 shows a more in depth scope of these tests.

Table 5: Regeneration Tests

Regeneration Test	Run	Regeneration Temperature (°C)	# of Vacuums
1	1	350	1
	2	200	1
	3	25	1
2	1	350	1
	2	25	1
	3	25	5

Regeneration test 1 consisted of three runs using a single sample. The first run was regeneration at 350°C and under vacuum. The second run was performed at a regeneration temperature of 200 °C and under vacuum. The third and final run involved only using vacuum evacuation for regeneration of the system. In all three runs, isotherm data was taken over a broad pressure range.

Regeneration test 2 also had three runs using a single sample of $AgNO_3/SiO_2$. The first run was once again regeneration at 350°C and under vacuum. The second run was a vacuum regeneration at room temperature (25 °C). The third run consisted of leaving the adsorbent overnight at an adsorption pressure of 10 atm. It was then regenerated using vacuum and once again brought back to a C_2H_4 pressure of 10 atm for adsorption. This was repeated five times and isotherm data was taken at the end of the 5^{th} regeneration. In all three runs, isotherm data was taken over a broad pressure range as well.

5. RESULTS & DISCUSSION

5.1 Constant Volume System $AgNO_3/SiO_2$ Regeneration Experimental Results

$AgNO_3/SiO_2$ has already been established in the literature as a viable option to further explore for commercial use of ethylene/ethane separations. That being said, the first experiments conducted for $AgNO_3/SiO_2$ were regeneration tests to further explore its viability as a commercial adsorbent for industrial purposes. Figures 7 and 8 reveal the results from the two regeneration tests conducted. The first test conducted as previously discussed was to explore the difference in capacity of the adsorbent after different regeneration temperatures. Ideally, there would be little to no difference between temperatures, indicating that lower temperatures could be used to regenerate the adsorbent. This in turn would lead to lower energy costs in preparing the adsorbent for industrial usage. Further more, little to no difference in capacity would also indicate that the adsorbent is reusable for more than one run. If it is only useful for a single run, then the savings in energy would be overturned to a cost in always changing the adsorbent, which would not make it a suitable candidate.

Figure 7 shows that when the adsorbent was regenerated after the fresh sample run was initially conducted; a slight drop off in capacity can be noted using the same regeneration temperature of 350 °C. The 2^{nd} regeneration at 200 °C yielded a capacity drop further below the initial and 2^{nd} runs. However, on the final run, taken after room temperature (25 °C) regeneration, it can be seen that the capacity was almost identical to that of the one observed after regeneration at 200 °C. This shows that there is no advantage of increasing the regeneration temperature between room temperature (25 °C) and 200 °C.

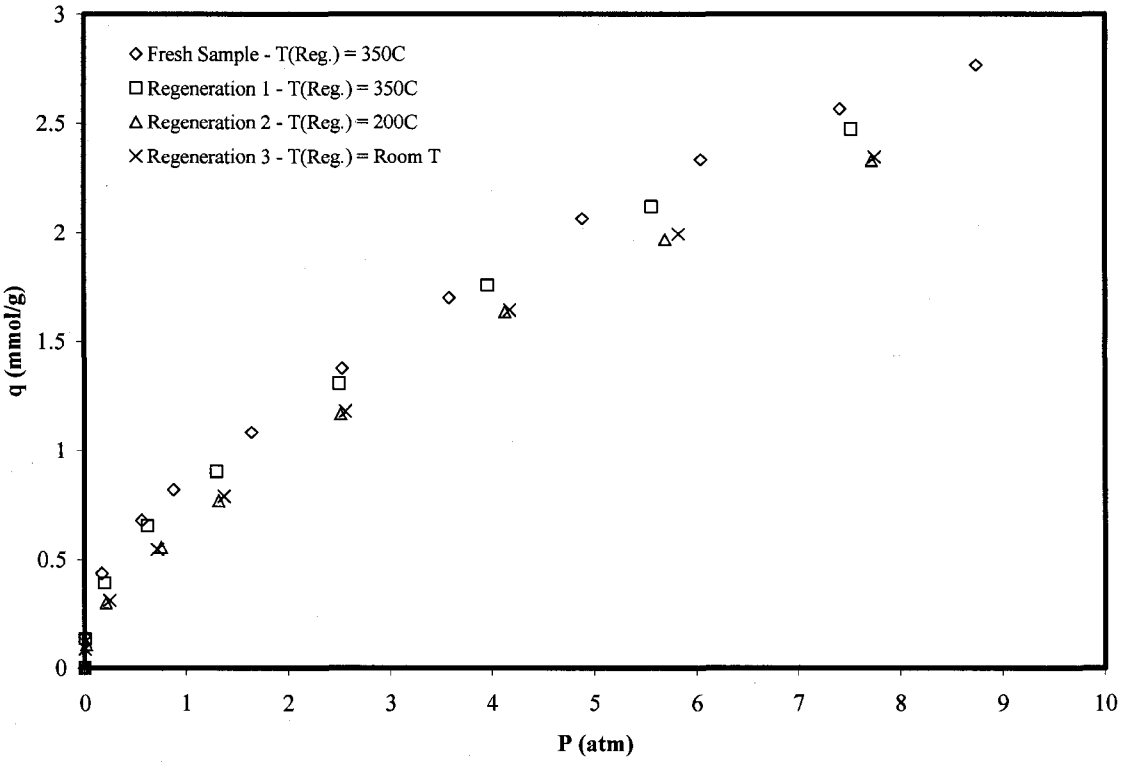

Figure 7: Isotherms for C_2H_4 at 34 °C with $AgNO_3/SiO_2$ Comparing Regeneration Temperature Effects

Figure 8 is the second test conducted in which the previous results were further explored to determine whether or not any temperature increase was necessary beyond the initial regeneration of the sample. First and foremost, the fresh sample values were compared to the previous values obtained with another sample to test for consistency. It can be seen that there is negligible difference between the old and new fresh sample values. The first regeneration was a single evacuation under room temperature (25 °C). A noticeable drop in the capacity is observed, especially at higher pressures, due to the temperature change for regeneration, as was observed in Figure 7. The second set of regeneration tests consisted of 5 consecutive vacuum regenerations at room temperature (25 °C) after saturating the adsorbent between regenerations, to simulate a more realistic use for the adsorbent in industry. This proved interesting in the fact that the performance

of the adsorbent seemed to improve slightly from the previous test. These results indicate that adsorption capacities observed after repeated regenerations at room temperature (25 °C) are very consistent. There is no need to go to high temperatures for the regeneration of $AgNO_3/SiO_2$. It may well be a plausible choice for industrial separation of ethane/ethylene mixtures. Padin & Yang (2000) and Rege & Yang (2002) have shown that adsorption can separate olefin/paraffin with promising results. The regeneration tests simply proved $AgNO_3/SiO_2$ has a reusable potential, which makes it that much more applicable to use within a commercial process.

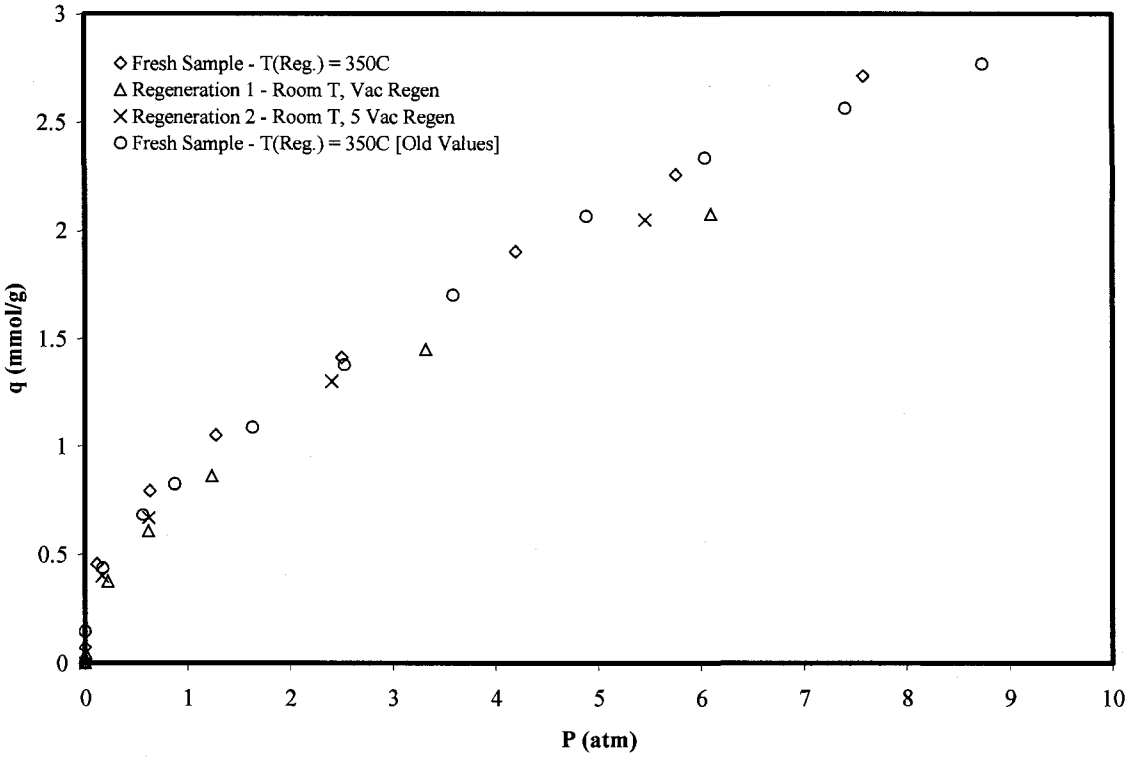

Figure 8: Isotherms for C_2H_4 at 34 °C with $AgNO_3/SiO_2$ Comparing Vacuum Regeneration Results

5.2 Determination of $CuCl/SiO_2$ Preparation Method Variables

As mentioned previously, $CuCl/SiO_2$ was considered as a potential choice for the ethane/ethylene separation discussed. However, unlike $AgNO_3/SiO_2$, there are no

experimental results discussed in literature claiming a specific ratio or preparation method of the adsorbent. Due to this lack of knowledge, it was determined that finding such a suitable method of preparation would be necessary before it was possible to compare the adsorbents. The combination of the two substances would not be as simple as using wet impregnation as it was in combining $AgNO_3/SiO_2$. There was no solvent found that CuCl was soluble in that SiO_2 had a high affinity for, as water was in the case of $AgNO_3$. This led to using a method referred to as monolayer thermal dispersion. An amount of CuCl was thoroughly mixed with SiO_2 and then heated to cause a fusion between the two substances. The heating would take place between 30 – 70% of the absolute melting point of CuCl. This is referred to as the Tammann temperature. A starting point of 412 °C was taken as a base temperature. This base temperature was taken from previous comparisons between wet thermal impregnation and monolayer thermal dispersion as methods for preparing $AgNO_3/SiO_2$ (Padin et al., 2000). Using this temperature, different mass ratios of CuCl: SiO_2, were taken to see if an optimal region could be found. Figure 9 yields these results as adsorption isotherms determined at 34 °C, with different mass ratios of $CuCl/SiO_2$. The measurement of uptake is taken as mmol adsorbate per g of total adsorbent.

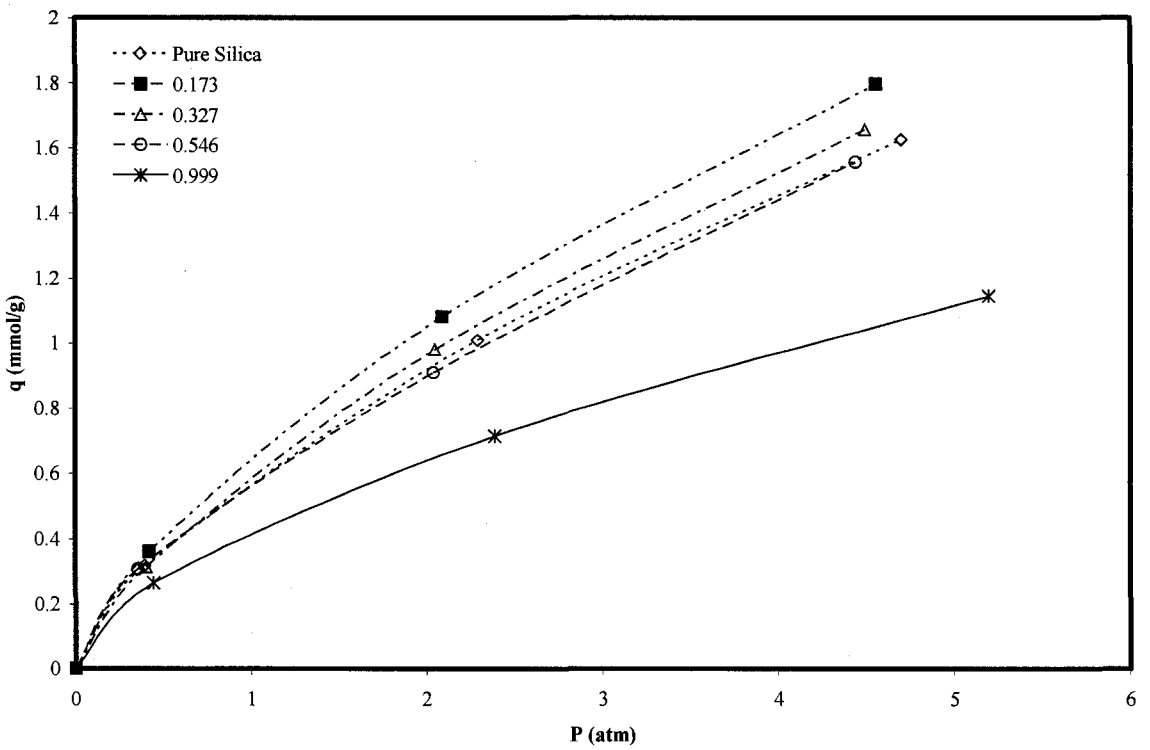

Figure 9: C_2H_4 at 34 °C on Differing Ratios of $CuCl/SiO_2$

It can be seen that 0.173 was the best ratio. In fact, when the ratio reached 0.546 g of CuCl, the performance of the prepared adsorbent was even lower than that of pure silica gel. This can be attributed to the fact that as more CuCl is added to the mixture, there is an increase in pore blockage within the silica gel. The CuCl is simply there to increase the attraction of the olefin to the adsorbent, but not to take up too much space within the pores.

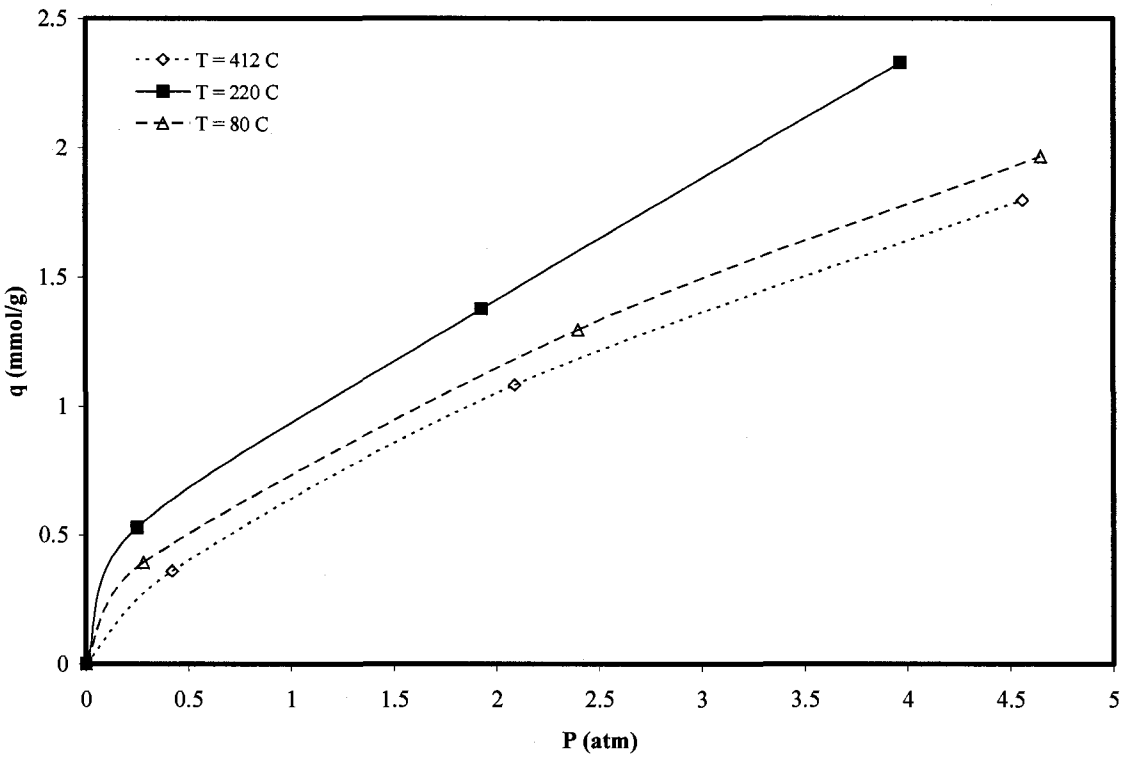

Figure 10: C_2H_4 at 34°C using 0.173:1 Ratio $CuCl/SiO_2$ with Different Preparation Temperatures

Once it was determined that 0.173g of CuCl was the best of the previous experiments, preparation temperature was looked at as well. Three temperatures were compared for the preparation of the sample. The previous test of 412°C was used, as well as 220°C, and 80°C. 220°C and 80°C was determined to be 70% and 50% of the absolute melting point (in Kelvin) of CuCl. Figure 10 shows the adsorption isotherms obtained at 34 °C for different preparation temperatures from the constant volume experiments. The ratios all being equal to 0.173, the preparation temperature that yielded the best results was 220°C. The previous experiments temperature of 412°C yielded the worst results. This could be accounted for by the fact that when heated that closely to the melting point (430°C), CuCl begins to block the pores of the silica gel due to its almost liquefied state. It is believed that while fusing the two substances is a must, when the temperature is that close to the melting point, an almost liquid CuCl will simply fill the pores, thus

decreasing capacity for adsorption. Therefore, all further experiments were conducted with the sample prepared at 220°C and with the ratio of 0.173 g CuCl to 1 g SiO_2. It should be noted that this is not necessarily the optimal preparation condition, but simply a rough starting point for the purpose of adsorbent comparison to follow.

5.3 Isotherms Obtained with Constant Volume System

Figures 11 – 13 give the adsorption isotherms obtained in the present study with the constant volume experiments conducted for the 3 adsorbents studied for ethylene and ethane as adsorbate, together with curve fits for 3 different adsorption isotherm models and comparison with the literature. A potential adsorbent would yield a close to linear isotherm characteristics with high slopes. If the isotherm yields a relatively linear trend, as opposed to a rectangular isotherm, this would mean that the difference between adsorption capacities for adsorption and desorption pressures would be higher for that specific adsorbent, which in turn will increase the efficiency of the regeneration. Any curvature would lead to a closer capacity difference between adsorption and desorption. This is especially relevant for a PSA system, in which the variable changed is the pressures to complete the process through desorption. It will be noted that Figure 11 contains both experimental data and literature. The 70°C isotherm data in Figure 11 is taken from Padin & Yang (2000). The literature data in Figure 11 does not reach the higher pressure conducted experimentally, but does give a comparison point to the experimental data for consistency.

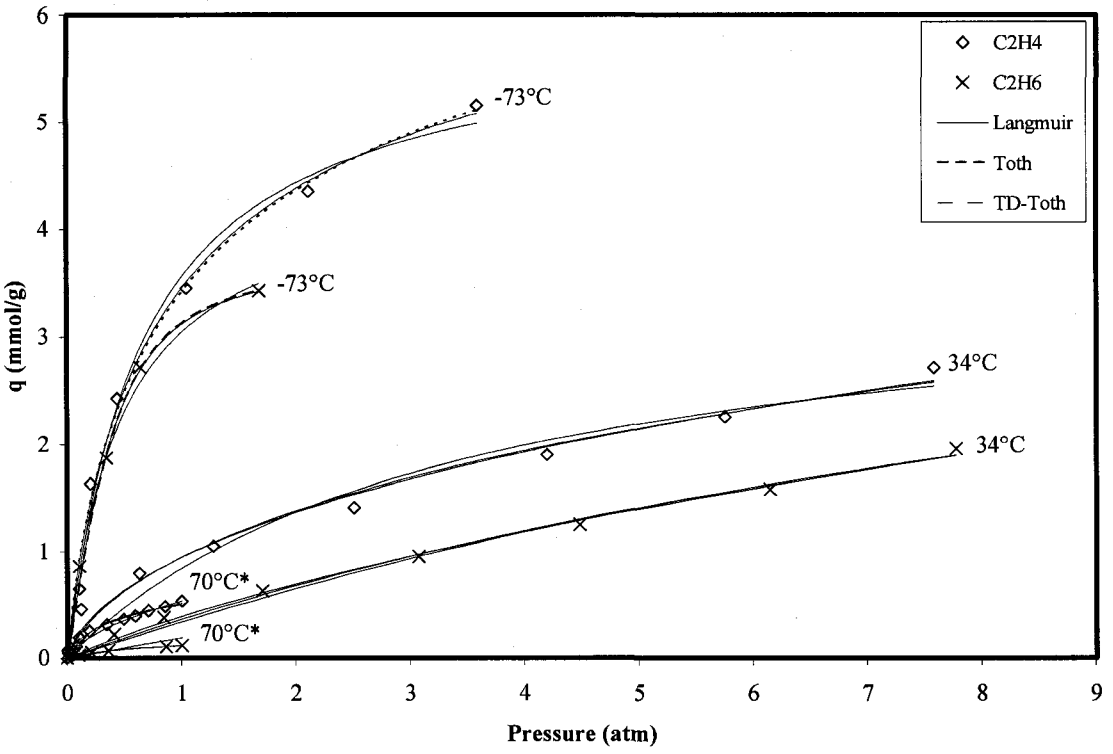

Figure 11: C_2H_4/C_2H_6 Isotherm Model Fits for $AgNO_3/SiO_2$ at Different Temperatures (*These values were plotted from Padin & Yang, 2000)

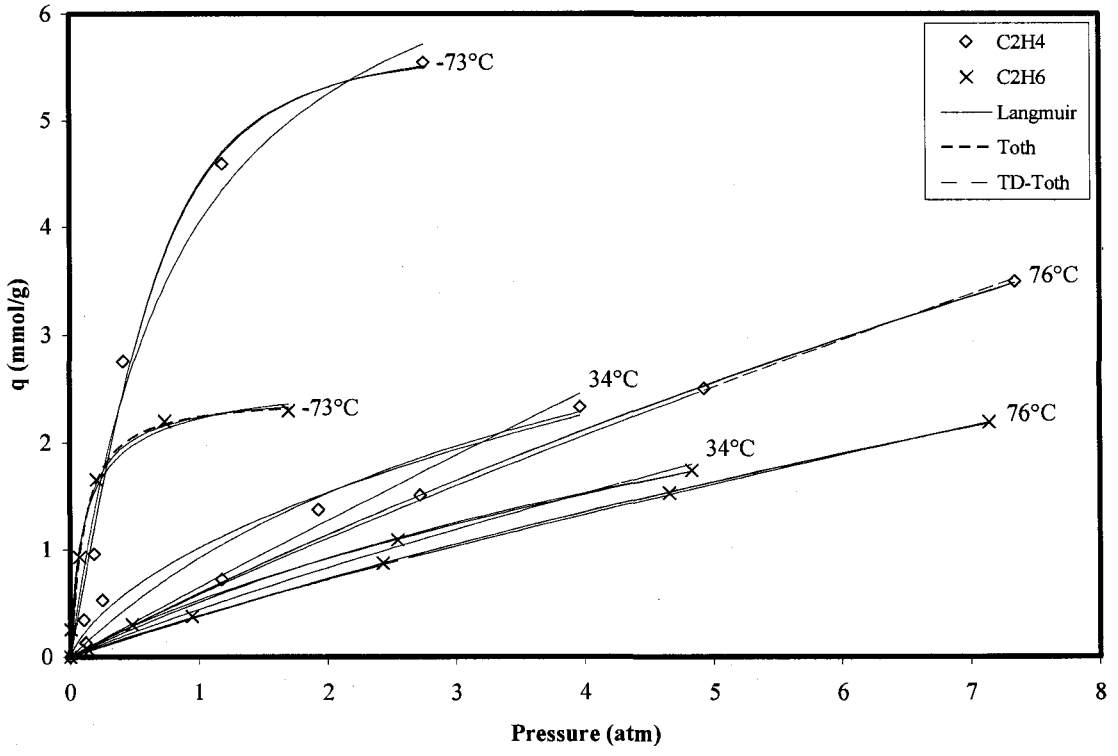

Figure 12: C_2H_4/C_2H_6 Isotherm Model Fits for $CuCl/SiO_2$ at Different Temperatures

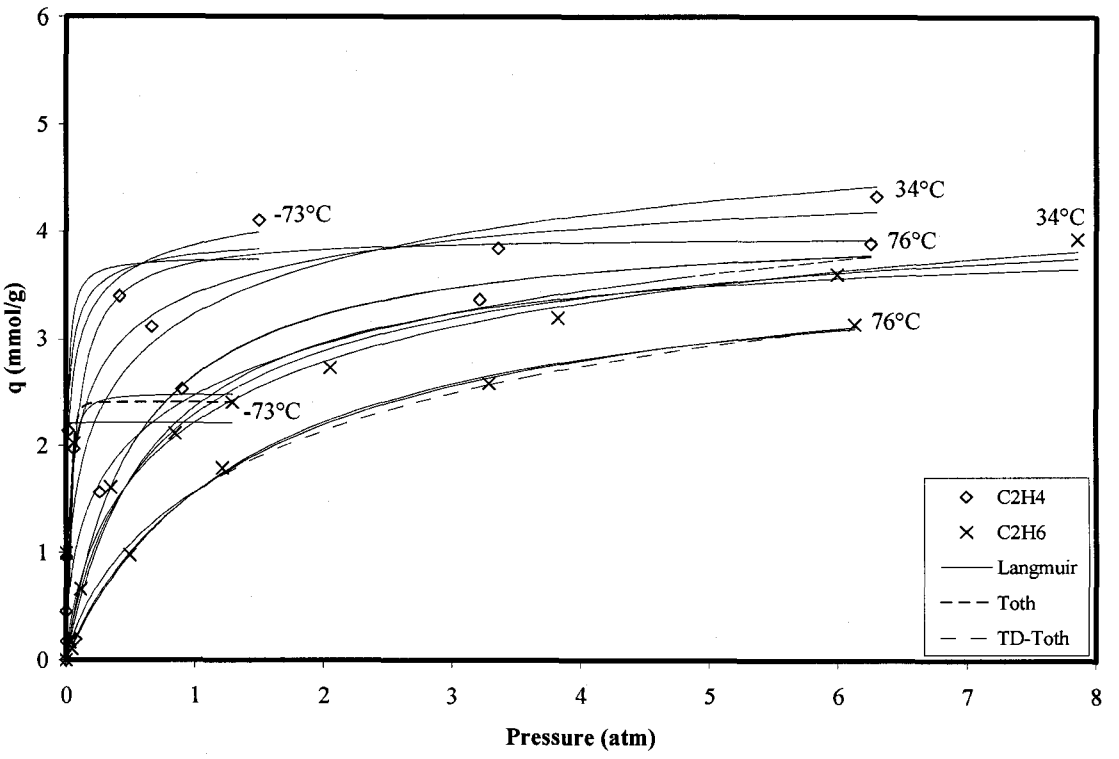

Figure 13: C_2H_4/C_2H_6 Isotherm Model Fits for CECA 13X at Different Temperatures

Comparing Figures 11-13 leads to few observations. The first one is that as temperature increases, the capacity of the adsorbents decrease for both ethylene and ethane, which is typical of physical adsorption. This is a fact due to adsorption being an exothermic process. $CuCl/SiO_2$ yielded the highest capacities of the three adsorbents for both ethylene and ethane at high pressures. As would be expected due to the molecular size and activity of the double bond, ethylene is adsorbed more by all three adsorbents studied. Furthermore, at temperatures above zero, both $AgNO_3/SiO_2$ and $CuCl/SiO_2$ yielded relatively linear trends. However, the rectangularity for both of these adsorbents at sub zero temperatures is a disadvantage, since the process in question would be conducted at sub zero temperatures. It would mean less of a capacity difference between the adsorption and desorption pressures, which would not be ideal for a PSA application.

Although, the initial results show a linear trend at lower pressures, it is the higher pressures that will need to be looked at when discussing the concept of industrial use of these adsorbents. Adsorption isotherms for CECA 13X for all the 3 temperatures studied were rectangular. The initial slope of the isotherm is quite linear, but that is at the lower pressures. The almost rectangular shape of the isotherms at all temperatures would not be suitable for PSA uses because at higher pressures there would be little capacity difference for desorption giving low expected working capacity for this adsorbent. The trend of linearity at higher pressures was found more so in $AgNO_3/SiO_2$ and $CuCl/SiO_2$ adsorbents at above zero temperatures.

5.4 Capillary Condensation Effects

It will be noted that all trends for subzero temperatures were found to show a plateau effect near the highest pressure used. This can be explained by the possibility of capillary condensation occurring within the adsorbents pores. Capillary condensation exists within a porous solid when multilayer adsorption of some vapour occurs to the point in which liquid from the gas phase begins to form within the pores (McNaught & Wilkinson, 1997). The Kelvin equation can be used to determine whether this phenomenon will have a real effect on the system. The Kelvin equation is as follows;

$$\ln\frac{p}{p_o} = \frac{2\gamma V_m}{rRT} \qquad [12]$$

The droplet radius, r, was estimated as 5 – 10% of the pore size of the 100 – 200 mesh silica gel used. Surface tension for both ethane and ethylene was found in Do & Ustinov (2003). The saturated vapour pressure, p_o, was then calculated. If the value calculated for p_o is smaller than p, then liquid will evaporate from the existing droplets. However, if p_o is greater than p, then the gas in the system will condense on the existing

droplets, increasing their size. An approximate calculation for both ethylene and ethane was conducted to study the possibility that capillary condensation affected the results of the subzero experiments. Table 6 shows the results of these calculations.

Table 6: Actual & Saturated Vapour Pressures of Ethylene/Ethane

Adsorbate	p (atm)	p_o (atm)
C_2H_4	4.51	4.48
C_2H_6	2.17	2.16

Table 6 shows that the values of the saturated vapour pressures are slightly below that of the actual vapour pressures of the adsorbate. This lends to the conclusion that the condensed liquid within the pores of the adsorbent will not collect more liquid, but will merely evaporate under those conditions. However, it can be argued that since the values are very close to each other that it is still very possible that the condensed gas will still likely collect within the pores, which would explain why there is such a plateau in the results when approaching the vapour pressure of the gas. Furthermore, without a measured pore radius value for the calculation, the accuracy of the calculations is affected.

5.5 Heat of Adsorption Results

When further examining the results of the isotherm fits, one can calculate the heat of adsorption for the adsorbents. By using $\frac{Q}{RT_o}$ from equation 5, found when fitting experimental data to the TD-Tóth model, one can calculate Q, the heat of adsorption. R is simply the gas constant and T_o is the lowest experimental temperature used. This would be an indication of how much energy would be necessary to desorb the adsorbate from the adsorbent. The lower the value, the more easily it is desorbed. Table 7 contains the values of these results.

Table 7: Heat of Adsorption for Different Adsorbent/Adsorbate Combinations

Adsorbate	Adsorbent	Q (kJ/mol)
C_2H_4	$AgNO_3/SiO_2$	7.35
	$CuCl/SiO_2$	26.61
	CECA 13X	7.082
C_2H_6	$AgNO_3/SiO_2$	14.38
	$CuCl/SiO_2$	45.75
	CECA 13X	11.93

As previously discussed, the higher the value of the heat of adsorption, the more energy intensive a separation would be. The values in Table 7 yield that $AgNO_3/SiO_2$ and $CuCl/SiO_2$ are both suitable candidates when comparing the large difference between the heats of adsorption for ethane and ethylene. In both cases, the values for ethane is almost double that of ethylene. In practical terms, that would mean that ethylene would be more readily desorbed than ethane, which is the exact result looked for when trying to produce a high purity ethylene product. However, the values found for $CuCl/SiO_2$ are much higher than that of the $AgNO_3/SiO_2$. This would mean that more energy would be required to simply separate the ethylene from the adsorbent. This is an example of an adsorbent having a higher capacity than its competitors; however, the energy savings may be offset by the higher cost to desorb the product from the adsorbent.

In comparison to Padin & Yang (2000), the values found in this study are quite different for ethylene/ethane. Padin & Yang reported heat of adsorption values for the ethane being less than that of ethylene using Zeolite 4A, Ag^+-Resin, and carbon molecular sieve. Practically speaking this makes sense because if an adsorbate is more adsorbed, there would be greater amounts of heat created. Therefore, the heats of adsorption would be larger. The method used to calculate the heat of adsorption for this study was the use of the variables $\frac{Q}{RT}$ in Equation 5 for the TD-Tóth trend fits. Based

on the variables found in those individual fits, the heat of adsorption was calculated. The method employed by Padin & Yang (2000) was a PSA computer simulation method using coupled differential equations.

5.6 Applicability of Isotherm Models

A visual examination of Figures 11 – 13 shows that the Tóth model fits very well compared to the other models. However, quantitative evidence is also necessary. A quantitative lack of fit test could not further prove that the Tóth equation was the best fit because the experiments performed are very difficult to conduct at the exact same pressures more than once for each temperature. There is too much variability in the x-value, which in this case is pressure. Since these replicates can not be produced, the lack of fit test could not be conducted. A simple comparison of the sum of squares of residuals (SSR) can still be used however. It can be seen in Tables 8 – 9 that the Tóth model yields the lowest values in practically all the fit comparisons. The lower the SSR value found, the more exact the fit. This further proves that the Tóth equation fits the data very well. It should also be noted that the other models did fit the data adequately as well.

Table 8: SSR Values for C_2H_4 Model Fits Using Various Temperatures & Adsorbents

Adsorbent	Temperature (°C)	Model	SSR
$AgNO_3/SiO_2$	-73	Langmuir	0.1619
		Toth	0.1200
		TD-Toth	0.2344
	34	Langmuir	0.2351
		Toth	0.0813
		TD-Toth	0.2344
	70	Langmuir	0.0052
		Toth	0.0016
		TD-Toth	0.2344
$CuCl/SiO_2$	-73	Langmuir	0.5523
		Toth	0.2576
		TD-Toth	0.4352
	34	Langmuir	0.0828
		Toth	0.0373
		TD-Toth	0.4352
	76	Langmuir	0.0053
		Toth	0.0047
		TD-Toth	0.4352
CECA 13X	-73	Langmuir	0.5358
		Toth	0.1082
		TD-Toth	1.3107
	34	Langmuir	0.4190
		Toth	0.0913
		TD-Toth	1.3107
	76	Langmuir	0.1757
		Toth	0.1756
		TD-Toth	1.3107

Table 9: SSR Values for C_2H_6 Model Fits Using Various Temperatures & Adsorbents

Adsorbent	Temperature (°C)	Model	SSR
$AgNO_3/SiO_2$	-73	Langmuir	0.0372
		Toth	0.0362
		TD-Toth	0.0565
	34	Langmuir	0.0021
		Toth	0.0003
		TD-Toth	0.0565
	76	Langmuir	0.0006
		Toth	0.0003
		TD-Toth	0.0565
$CuCl/SiO_2$	-73	Langmuir	0.0372
		Toth	0.0362
		TD-Toth	0.0565
	34	Langmuir	0.0021
		Toth	0.0003
		TD-Toth	0.0565
	76	Langmuir	0.0006
		Toth	0.0003
		TD-Toth	0.0565
CECA 13X	-73	Langmuir	0.0740
		Toth	0.9781
		TD-Toth	1.1675
	34	Langmuir	0.2537
		Toth	0.0982
		TD-Toth	1.1675
	76	Langmuir	0.0088
		Toth	0.0075
		TD-Toth	1.1675

5.7 Binary Isotherm Prediction

For all constant volume isotherms collected, the data reflects a pure component system. These values do not represent any binary mixture behaviour that would occur during industrial use of the adsorbents studied. Binary behaviour would include competitive adsorption. Based on the pure component results, there is potential for competitive adsorption to play a large role in the adsorbent efficiency. Both ethane and ethylene are adsorbed fairly well by all three adsorbents and may not yield as promising

results when competitive adsorption is encountered. Using the IAST model, the binary behaviour of ethane/ethylene was predicted for all 3 adsorbents at 34 °C using the pure component Langmuir model fits used in §5.3. The subzero conditions were not modelled because at -73 °C and at high pressures, the system is no longer in the gas phase. Figures 14 – 16 show the results of the IAST binary predictions.

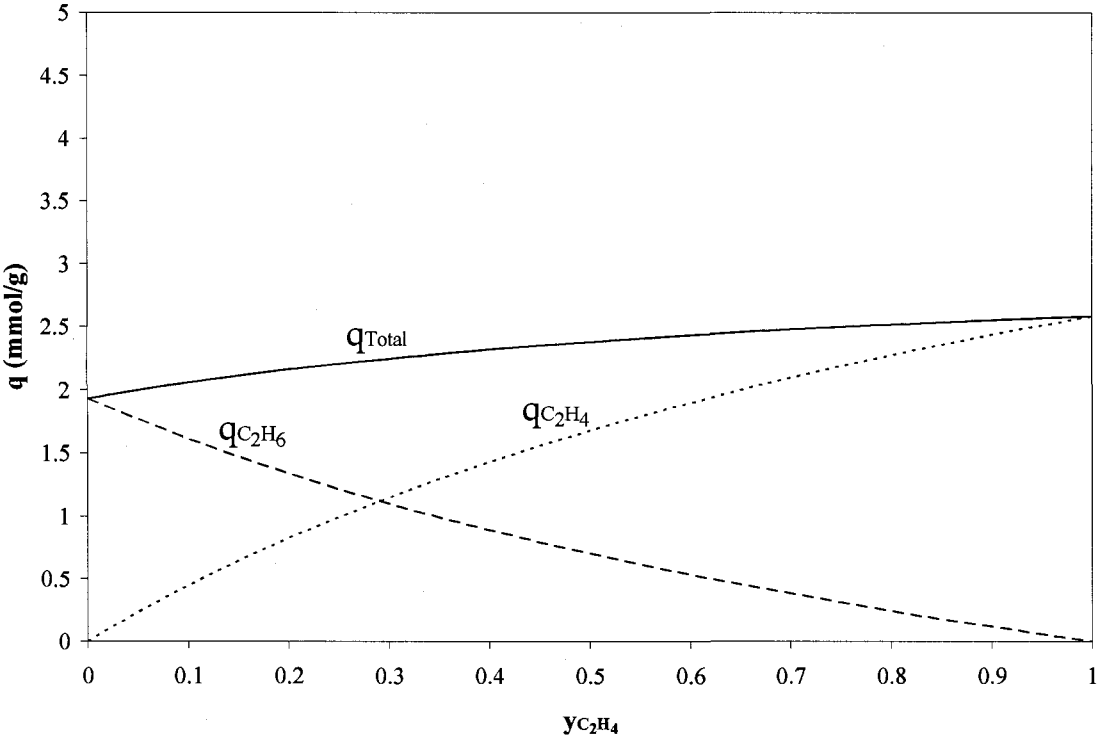

Figure 14: IAST Model Prediction for C_2H_4/C_2H_6 Mixture using $AgNO_3/SiO_2$ at 34°C & 8atm

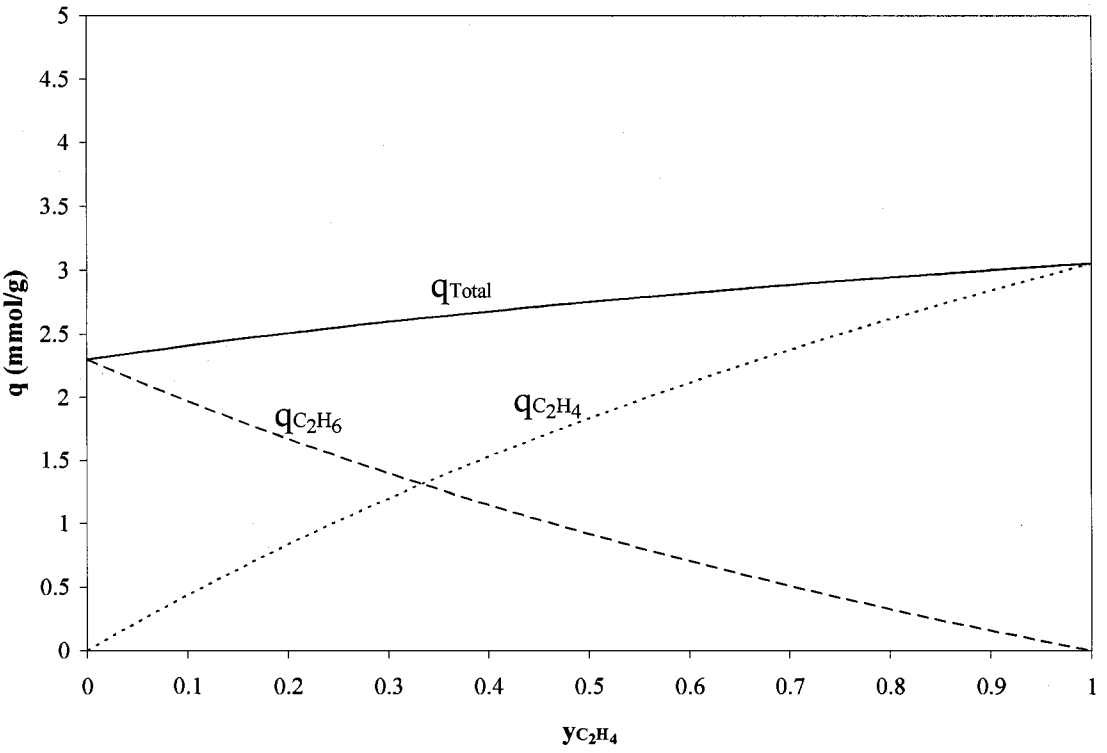

Figure 15: IAST Model Prediction for C_2H_4/C_2H_6 Mixture using $CuCl/SiO_2$ at 34°C & 8atm

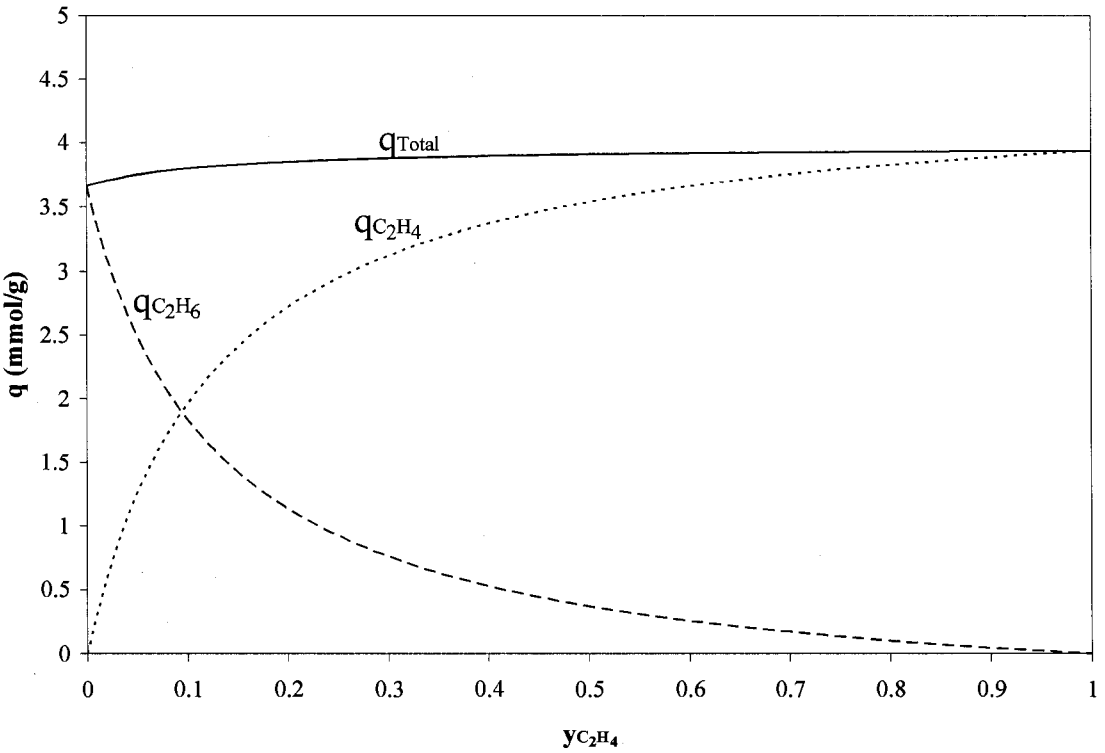

Figure 16: IAST Model Prediction for C_2H_4/C_2H_6 Mixture using CECA 13X at 34°C & 8atm

The comparison of the three figures yields a promising result for $CuCl/SiO_2$. At above the 50/50 mixture of ethane/ethylene, Figure 15 shows that $CuCl/SiO_2$ has a growing difference between the capacities of ethane adsorbed versus that of ethylene. Ethylene is adsorbed at a continuously growing rate from a 50/50 mixture of ethylene/ethane to a pure ethylene situation. The results of $AgNO_3/SiO_2$, although promising as well, do not achieve the same result as the prediction for $CuCl/SiO_2$. Similar results would be expected at lower temperatures based on inspection of the pure component data. CECA 13X results seem to yield very promising results. However, based on inspection of the pure component data, it is seen that the system is too rectangular for such a separation.

Phase diagrams were used to compare the separation of ethylene from the binary mixture for the 3 adsorbents modelled above. This is slightly different than the typical phase diagram that represents vapour-liquid equilibrium. For adsorption purposes, the x-axis represents ethylene still in the gas phase and the y-axis represents ethylene adsorbed. When the equilibrium line (dashed line) is above the 45° line (solid line), the separation is favourable. The further above it is, the more favourable the separation becomes. The temperature used was once again 34°C and the pressure was 8atm. Figures 17 – 19 display the results.

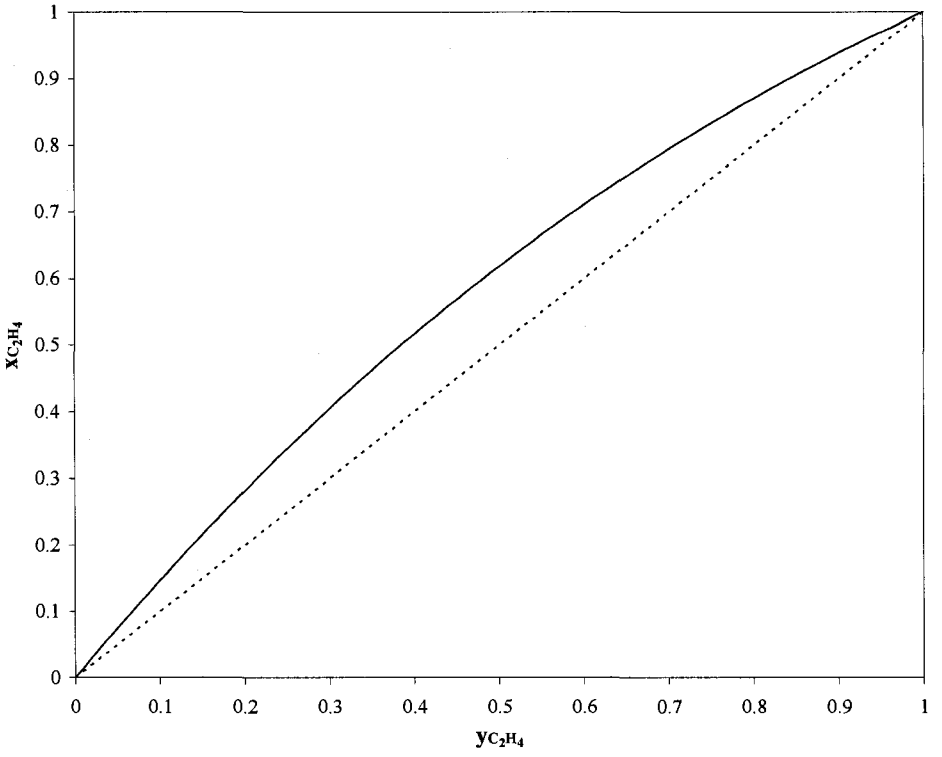

Figure 17: Phase Diagram for C_2H_4/C_2H_6 using $AgNO_3/SiO_2$ at 34°C & 8atm

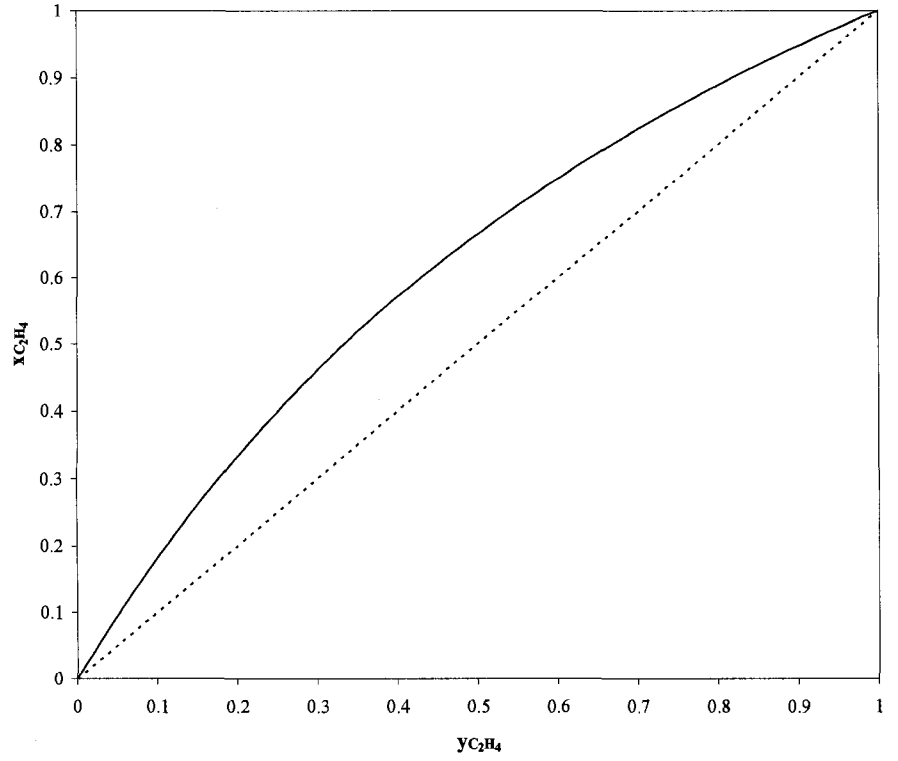

Figure 18: Phase Diagram for C_2H_4/C_2H_6 using $CuCl/SiO_2$ at 34°C & 8atm

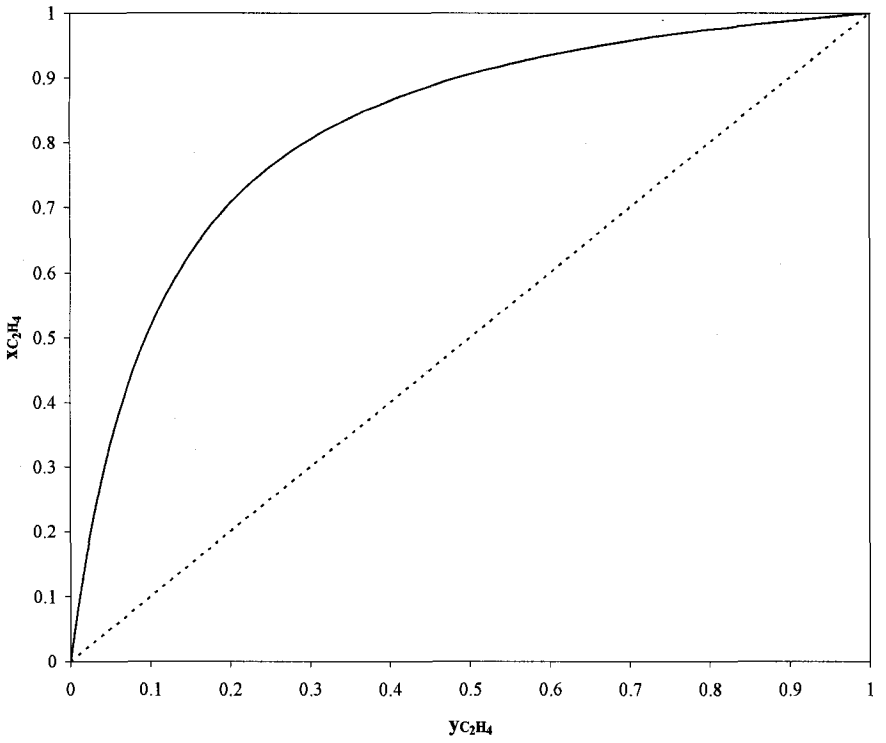

Figure 19: Phase Diagram for C_2H_4/C_2H_6 using CECA 13X at 34°C & 8atm

When examining Figures 17 – 19, it can be seen clearly that $CuCl/SiO_2$ once again outperforms the other two adsorbents. Both $AgNO_3/SiO_2$ and $CuCl/SiO_2$ yield favourable separation results, but $CuCl/SiO_2$ has a larger separation from the line of equilibrium. This lends to the idea that $CuCl/SiO_2$ would have separate ethylene from a binary mixture of ethane/ethylene more efficiently. CECA 13X showed once again that using it for this application would not be a viable option. If using CECA 13X, the phase diagram shows that separation would be more difficult. $CuCl/SiO_2$ shows some real potential for binary mixture separation of ethane/ethylene based on the previous results.

5.8 Expected Working Capacity

The expected working capacity (EWC) of any process is a vital indication of its efficiency. In terms of adsorption processes (PSA, VSA, TSA), the expected working

capacity indicates the difference between the capacities of adsorption and desorption conditions. This allows for an indication of how much the process itself can recover. Equation [13] is used to calculate the EWC;

$$Expected\ Working\ Capacity(EWC) = q_{adsorption} - q_{desorption} \qquad [13]$$

EWC will vary depending on the operating conditions used. The larger the difference between the pressures in PSA and VSA, the higher the EWC is going to be. The lower desorption pressure is compared to the adsorption pressure, the higher the EWC becomes. In the case of TSA, the higher the desorption temperature is in comparison to the adsorption temperature, the lower the capacity for desorption becomes. This yields a higher difference in capacity between adsorption and desorption, thus yielding a higher EWC, which will increase the recovery during the desorption process.

Figures 20 – 22 show the results of EWC calculations for ethylene and ethane. The adsorption pressure was taken from 1 – 8 atm, while desorption pressure was taken arbitrarily as 1 atm. This is under the assumption that only one PSA would be used in this process. In reality, there is the possibility that more than one pair of PSA columns will be employed. If this is the case, a higher desorption pressure may be used initially so that the product can be sent in to the next columns with the possibility of further purification. If the pressure is too low going in to the next adsorption columns, there may not be a large enough difference between the adsorption and desorption capacities to further purify the product effectively. The only way it could be performed in a single step is if the desorption pressure chosen could effectively obtain the exact concentration of the desired product. This may not be the case however in this scenario.

The model used to calculate the capacities was the Tóth model because as previously established, it was the best fit of the three models chosen. It should be noted that these values were chosen because this was the range of the constant volume experiments which yielded the model fits used for the EWC calculation. It is possible to extrapolate much higher pressures, but the values would not necessarily yield realistic values and simply be an extension of the experimental trend established. Furthermore, these values represent pure system expected working capacity. The values are based on pure component data, thus competitive adsorption was not considered in these calculations.

While examining the EWC figures, it can be seen that as pressure increases, so do the individual EWC values. This is to be expected since as pressure increases, so then does the capacity of an adsorbent. The sub-zero temperature values are of much greater interest, based on the fact that the temperatures in industry would be within the sub-zero region. $AgNO_3/SiO_2$ yields the greatest EWC for ethylene under these conditions. This means it displays through this calculation, the highest recovery potential for ethylene. Once again, CECA 13X yields unfavourable results, as expected from the shape of its isotherms. In some cases, it displays a higher EWC for ethane than ethylene, which is not the aim for this project. $CuCl/SiO_2$ yields a EWC for ethylene that reaches about half of $AgNO_3/SiO_2$ at sub-zero temperatures.

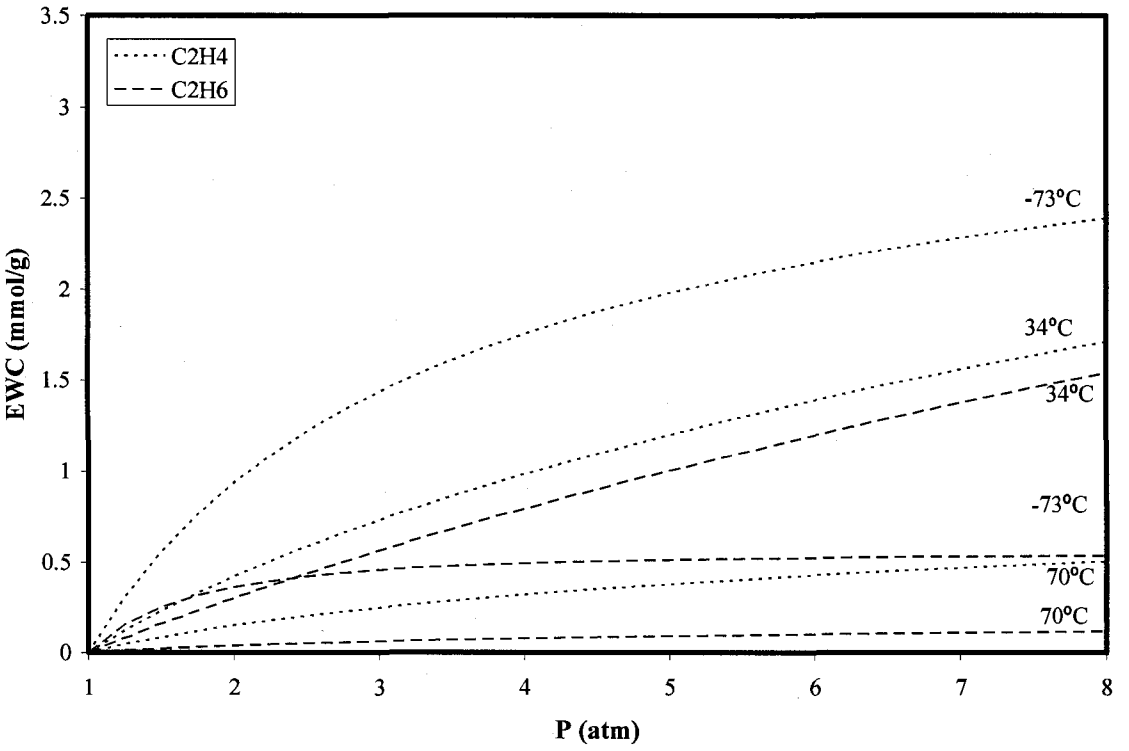

Figure 20: Expected Working Capacity for $AgNO_3/SiO_2$ as a function of the Adsorption Pressure, P, at Varied Temperatures for PSA with Desorption at P = 1 atm

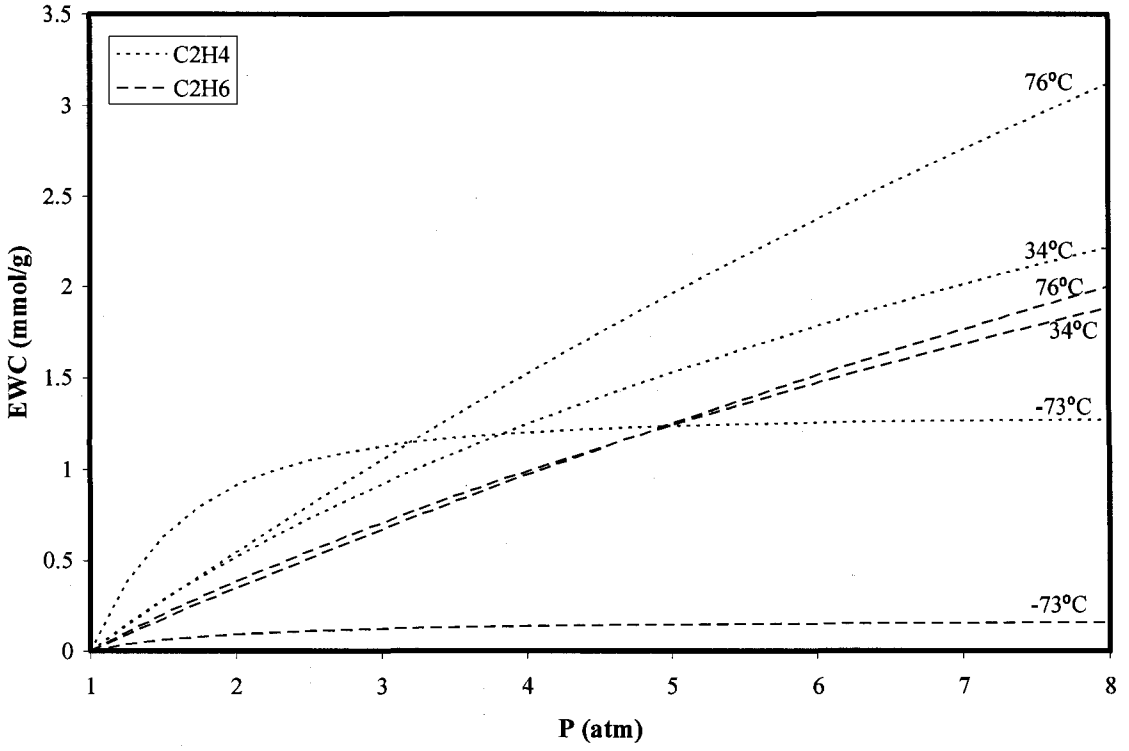

Figure 21: Expected Working Capacity for $CuCl/SiO_2$ as a function of the Adsorption Pressure, P, at Varied Temperatures for PSA with Desorption at P = 1 atm

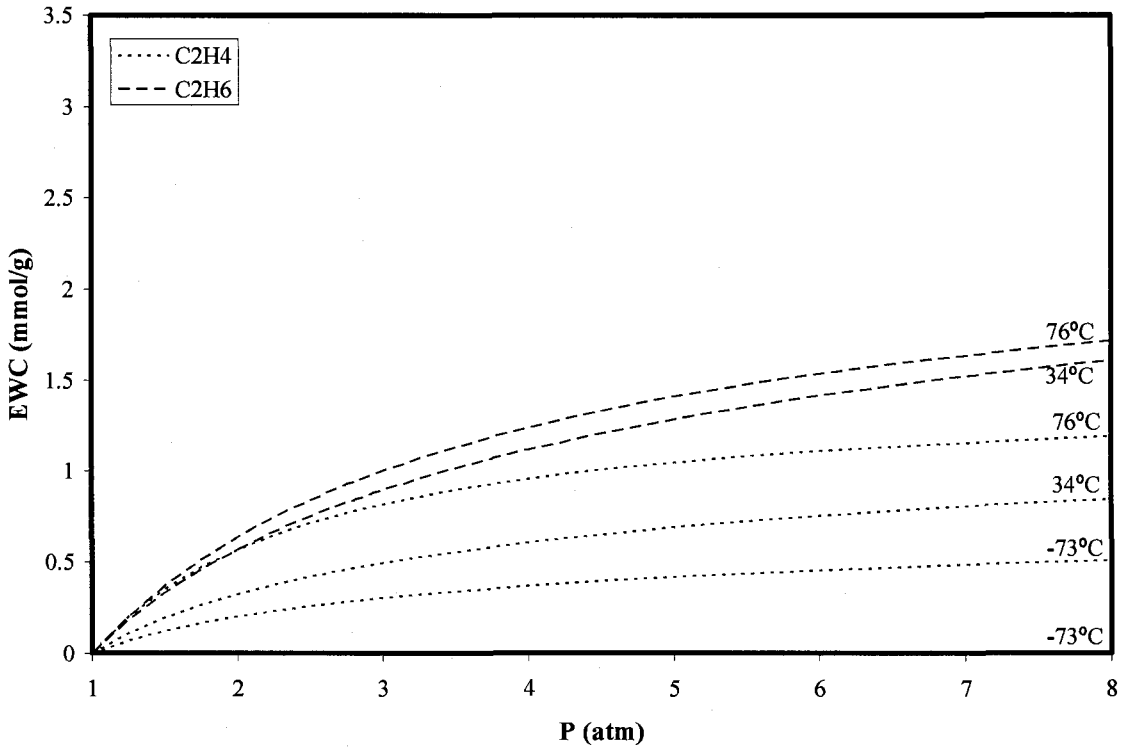

Figure 22: Expected Working Capacity for CECA 13X as a function of the Adsorption Pressure, P, at Varied Temperatures for PSA with Desorption at P = 1 atm

Figures 20 – 22 show the EWC on an individual component basis at varied temperatures. A further indication of the performance of the adsorbents would be the difference between the EWC for the individual adsorbate themselves at the same temperatures. A comparison of the EWC difference between the individual components is of much more interest. As an extension of these figures, Figures 23 – 25 show the results of these calculations. The EWC for ethane was subtracted from that of ethylene to calculate the difference. If a positive number was yielded, more ethylene was recovered than ethane. Likewise, if negative values were yielded, more ethane was recovered.

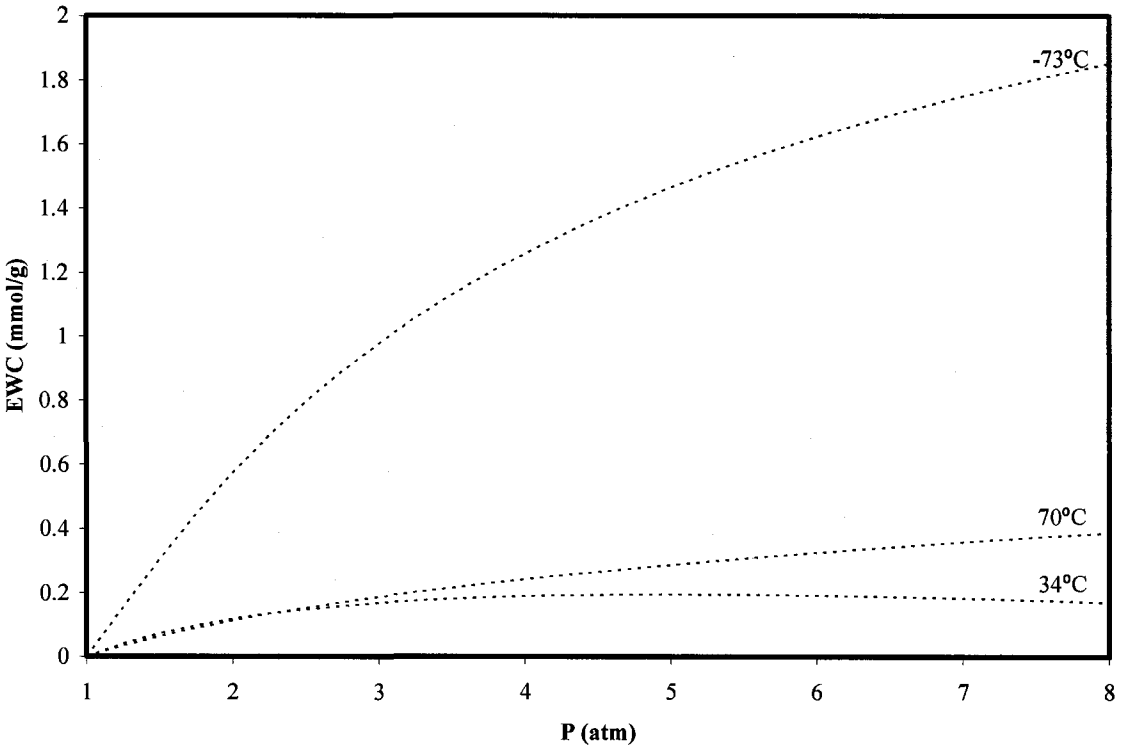

Figure 23: Expected Working Capacity Difference between C_2H_4/C_2H_6 for $AgNO_3/SiO_2$

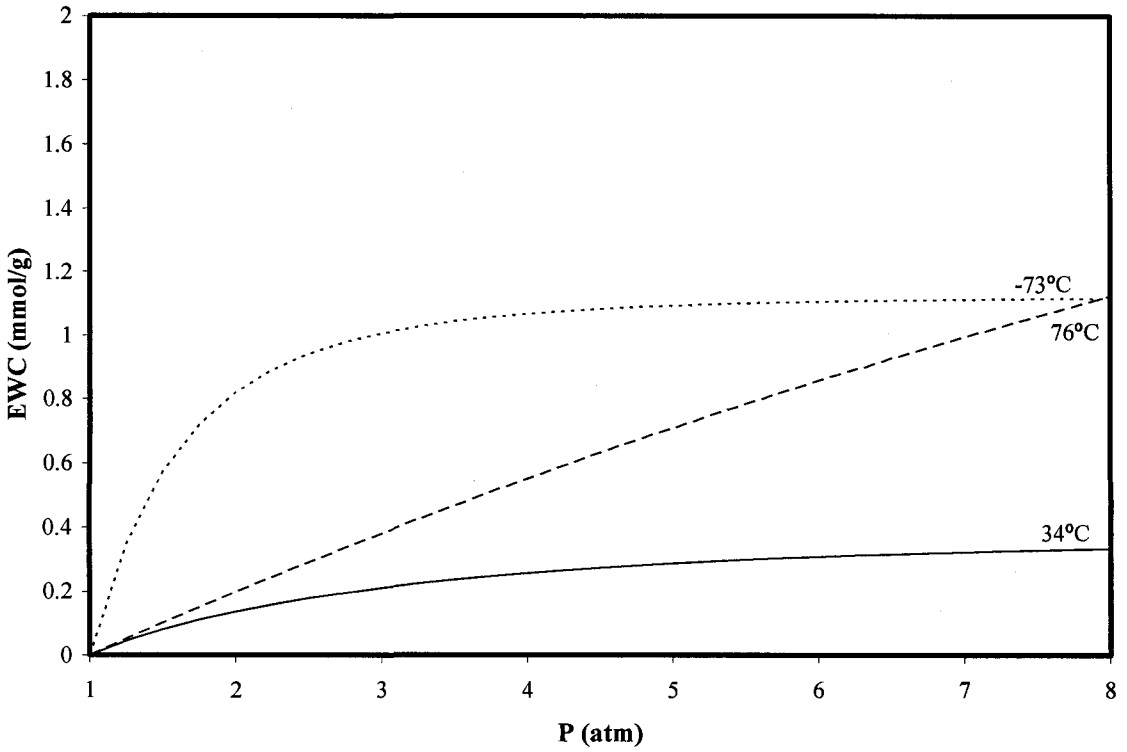

Figure 24: Expected Working Capacity Difference between C_2H_4/C_2H_6 for $CuCl/SiO_2$

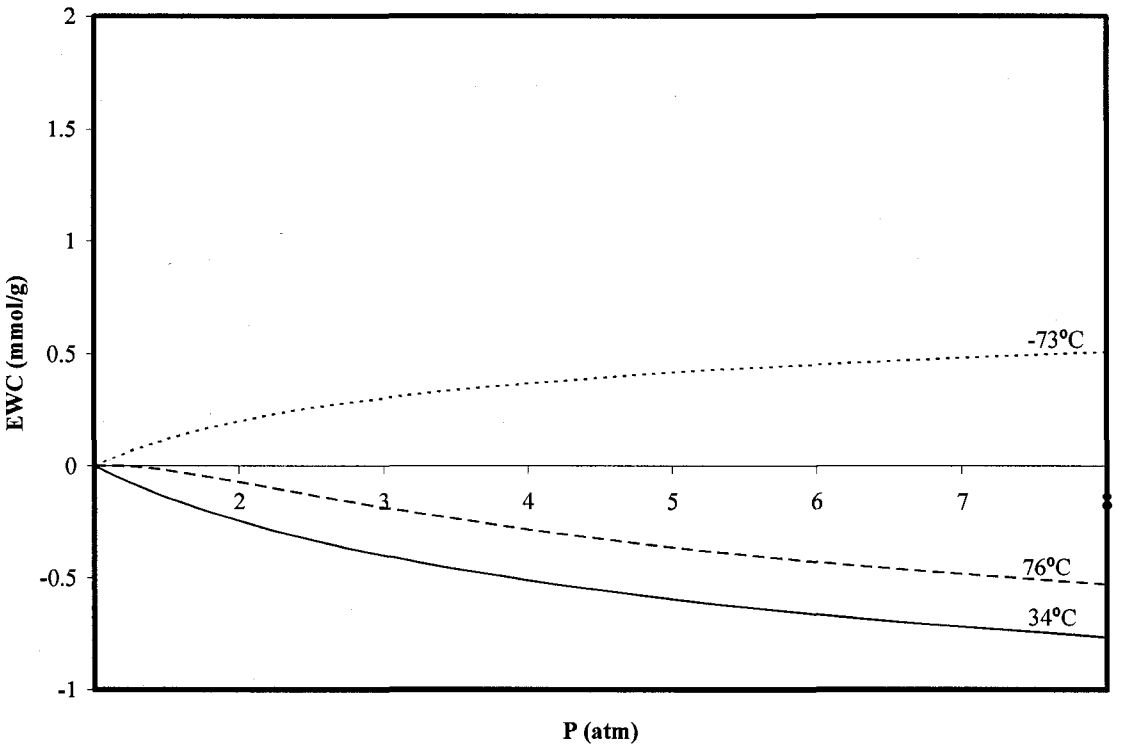

Figure 25: Expected Working Capacity Difference between C_2H_4/C_2H_6 for CECA 13X

It can be easily seen from these figures that $AgNO_3/SiO_2$ yields the best results in terms of EWC differences at the sub-zero temperature compared to the rest. $CuCl/SiO_2$ yields better overall results in terms of EWC differences at all temperatures however. In both these cases, more ethylene is recovered than ethane. This would mean that if a PSA were employed, during desorption more ethylene could be recovered as a result of there being a higher amount within the pores of the adsorbent. Yielding a higher concentration of ethylene in the product stream is the goal for this project, since that is the desired product in the end. As discussed previously, it is likely that a few PSA systems would be necessary to obtain the desired concentration. However, it can be seen that more ethylene would be recovered in each cycle used. Based on the results shown in Figures 20-22, CECA 13X seems to yield a higher recovery of ethane, than ethylene however. This is not the result being sought after for the separation application in question. This result is

simply a further indication that CECA 13X may not be a suitable choice for this type of application, which has been previously shown with other zeolites in literature.

5.9 Economic Analysis

An economic analysis was performed for the individual adsorbents to roughly calculate the cost of the addition of a pressure swing adsorption unit to an already existing cryogenic distillation column to be used as a hybrid process. Using the specifications given from industry, the TD-Tóth model was used to calculate the exact capacities of each adsorbent under the specific conditions in question. The column volume was calculated based on the volume of adsorbent necessary to adsorb the desired amount of ethylene. A worst case recovery scenario of 50% was used. Competitive adsorption was not considered in this case study. It is noted that this calculation assumes that the amount of ethane adsorbed and recovered is negligible for simplification purposes. It was seen that both ethylene and ethane would be significantly adsorbed, but as a starting point, ethane adsorption was deemed negligible.

Furthermore, using an L/D ratio for adsorption of 5, the column height and diameter could then be calculated. The adsorbent cost was calculated using a quoted value from industry. The column cost was calculated using standardized plant design equations (Geankoplis, 2003). The recycling of the stream that remains unadsorbed being considered, a compression cost was included in the analysis, but is not shown. Most of the energy costs would come from pressurizing the system, but because the feed comes in at a high pressure already, this is not necessary to calculate. Furthermore, provided that the ethylene product is not needed at a higher pressure than what it is desorbed at, there is no cost of pressurizing the product incurred. Table 10 shows the

results of this analysis for a single continuous adsorption unit. This consists of two columns, both filled with adsorbent. For in depth calculations, refer to §A of the appendix.

Table 10: Economic Analysis Comparison of Different Adsorbents

Adsorbent	Column Cost	Adsorbent Amount (kg)	Adsorbent Cost	Total Cost
$AgNO_3/SiO_2$	$669 374	3539.05	$1 099 259	$1 768 633
$CuCl/SiO_2$	$560 483	707.50	$236 904	$797 388
CECA 13X	$ 1 150 606	27198.40	$1 250 336	$2 400 941

Based on the calculation described, it can be seen in Table 10 that $CuCl/SiO_2$ is a much cheaper alternative than the other two adsorbents, with CECA 13X coming out as the most expensive alternative. Due to its higher capacity, $CuCl/SiO_2$ would need less adsorbent amount to adsorb the necessary amount of ethylene, in comparison to the others.

6. CONCLUSIONS & RECOMMENDATIONS

$CuCl/SiO_2$ was determined to have the best results during the constant volume experiments. It also showed promising results when the binary predictions were conducted. It clearly outperformed both $AgNO_3/SiO_2$ and CECA 13X in a more realistic industrial situation of an ethane/ethylene mixture. It would be further necessary however, to optimize the preparation conditions for $CuCl/SiO_2$ to explore the potential of this adsorbent. When comparing the heats of adsorption however, the values found for $AgNO_3/SiO_2$ were determined to be the most favourable for the proposed process. For ethylene and ethane, the values were 7.35 kJ/mol and 14.38 kJ/mol, respectively. Furthermore, when comparing the EWC of the individual adsorbents, $AgNO_3/SiO_2$ was found to have the best capacity difference at sub-zero temperatures between the individual adsorbate. An economic analysis revealed that $CuCl/SiO_2$ would potentially be the lowest costing adsorbate to utilize in industry. This was based on strictly looking at the adsorption and recovery of C_2H_4.

From the data obtained in this work, it can be stated that both $AgNO_3/SiO_2$ and $CuCl/SiO_2$ have a favourable potential for the possible use in industry as an energy saving addition to separating ethylene and ethane. Recommended works for the future include higher pressure constant volume experimentation, as well as further optimizing the preparation of $CuCl/SiO_2$. Experimental binary results for ethylene/ethane would further indicate the behaviour of the system, which is necessary for any further progress. Binary experiments would be necessary to study the competitive adsorption that would most definitely be a factor. This is assumed based on the quantity of both adsorbents that

is adsorbed during pure component experiments. This was further emphasized by the binary predictions performed in this work.

7. LIST OF REFERENCES

1. Blas, F.J., Vega, L.F., Gubbins, K.E. (1998). Modeling new adsorbents for ethylene/ethane separations by adsorption via π-complexation. Fluid Phase Equilibria, Vol. 150, Issue 151, 117 - 124

2. Choi, B., Choi, D., Lee, Y., Lee, B. (2003). Adsorption Equilibria of Methane, Ethane, Ethylene, Nitrogen, and Hydrogen onto Activated Carbon. J. Chem. Eng. Data, 48, 603 – 607

3. CECA Specialty Chemicals. (2008). Natural Gas and NGL Sweetening, http://www.cecachemicals.com/sites/ceca/en/business/molecular_sieves/natural_gas/natural_gas_ngl_sweetening.page

4. Chen, N., Yang, R.T. (1996). Ab initio Molecular Orbital Study of Adsorption of Oxygen, Nitrogen, and Ethylene on Silver-Zeolite and Silver Halides. Ind. Eng. Chem. Res., 35, 4020 – 4027

5. Cheng, L.S., Yang, R.T. (1995). Monolayer Cuprous Chloride Dispersed on Pillared Clays for Olefin-Paraffin Separations by π-Complexation. Adsorption, 1, 61 – 75

6. Choudary, V.R., Mayadevi, S. (1993). Adsorption of Methane, Ethane, Ethylene, and Carbon Dioxide on High Silica Pentasil Zeolites and Zeolite-like Materials Using Gas Chromatography Pulse Technique. Separation Science and Technology, 28 (13 & 14), 2197 – 2209

7. Do, D.D., Ustinov, E., Do, H.D. (2003). Phase equilibria and surface tension of pure fluids using a molecular layer structure theory (MLST) model. Fluid Phase Equilibria, 204, 309 – 326.

8. Eldridge, R.B. (1993). Olefin/Paraffin Separation Technology: A Review. Ind. Eng. Chem. Res., 32, 2208 – 2212

9. Geankoplis, C.J. (2003). Transport Processes and Unit Operations, 4th Ed., Prentice –Hall Inc.

10. Humphrey, J.L., Seibert, A.F., Koort, R.A. (1991). "Separations Technologies Advances and Priorities", U.S. Department of Energy Report, 12920-1

11. King, C.J. (1987). Separation processes based on reversible chemical complexation. In R. W. Rousseau, Handbook of separation process technology. New York: Wiley.

12. McNaught, A.D., Wilkinson, A. (1997). Compendium of Chemical Terminology, 2nd. Blackwell Science.

13. IPCS InChem. (2005) Ethylene (Screening Information Data Set - SIDs). http://www.inchem.org/documents/sids/sids/74851.pdf .

14. Ng, W.K., Kolmetz, K., Lee, S.H., Cook, C.G. (2005). Energy Optimization of Cryogenic Distillation. 2005 Spring A.I.Che. Meeting.

15. Padin, J., Yang, R.T. (2000). New sorbents for olefin/paraffin separations by adsorption via π-complexation: synthesis and effects of substrates. Chemical Engineering Science, 55, 2607 – 2616

16. Rege, S.U., Padin, J., Yang, R.T. (1998). Olefin/paraffin separations by adsorption: π-complexation vs. kinetic separation. AIChE Journal, 44, 799 – 809

17. Rege, S.U., Yang, R.T. (2002). Propane/propylene separation by pressure-swing adsorption: sorbent comparison and multiplicity of cyclic steady states. Chemical Engineering Science, 57, 1139 – 1149

18. Ren, T., Patel, M., Blok, K. (2006). Olefins from conventional and heavy feedstocks: Energy use in steam cracking and alternative processes. Energy, 31, 425 – 451

19. Ruthven, D.M. (1984). Principles of Adsorption and Adsorption Processes. John Wiley & Sons Inc., New York, NY. 1-433.

20. Speight, J.E. (1991), The Chemistry And Technology Of Petroleum. Marcel Dekker, Inc., 219 – 226

21. Suzuki, M. (1990). Adsorption Engineering. Kodansha LTD., 5.

22. Tóth, J. (2002). Adsorption: Theory, Modeling, and Analysis. New York: Marcel Dekker Inc.

23. Wu, Z., Han, S., Cho, S., Kim, J., Chue, K., Yang, R.T. (1997). Modification of Resin-Type Adsorbents for Ethane/Ethylene Separation. Ind. Eng. Chem. Res., 36, 2749 – 2756

24. Yang, R.T. (2003). Adsorbents: Fundamentals and Applications. Hoboken, N.J. Wiley Interscience

8. NOMENCLATURE

b	Affinity	[atm^{-1}]
b_i	Affinity of Component I	[atm^{-1}]
b_j	Affinity of Component j	[atm^{-1}]
b_o	Affinity at Reference Temperature	[atm^{-1}]
c	Higher Adsorbed Component	[-]
d	Lower Adsorbed Component	[-]
p	Actual Vapour Pressure	[atm]
p_o	Saturation Vapour Pressure	[atm]
P	Pressure	[atm]
q	Adsorption Capacity	$[\frac{mmol}{g}]$
$q_{adsorption}$	Capacity During Adsorption	$[\frac{mmol}{g}]$
$q_{desorption}$	Capacity During Desorption	$[\frac{mmol}{g}]$
$q_{s,o}$	Maximum Adsorption Capacity at Reference Temperature	$[\frac{mmol}{g}]$
q_i	Adsorption Capacity of Component I	$[\frac{mmol}{g}]$
q_s	Maximum Adsorption Capacity	$[\frac{mmol}{g}]$
$q_{s,i}$	Maximum Adsorption Capacity of Component i	$[\frac{mmol}{g}]$
Q	Heat of Adsorption	$[\frac{J}{mol}]$

r	Droplet Radius	[μm]
R	Gas Constant (8.314)	$[\frac{J}{mol \cdot K}]$
s	Experimental Value	$[\frac{mmol}{g}]$
$\hat{s}$	Calculated Value	$[\frac{mmol}{g}]$
t	Tóth Constant	[-]
T	Temperature	[°C or K]
T_o	Reference Temperature	[°C or K]
V_m	Molar Volume	$[\frac{m^3}{mol}]$
x	Equilibrium Mole Fraction in Adsorbed Phase (Still Gas)	[-]
y	Equilibrium Mole Fraction in Gas Phase	[-]
y_i	Gas Phase Composition of Component i	[-]
y_j	Gas Phase Composition of Component j	[-]
Greek Letters		
α	TD – Tóth Constant	[-]
α_{ij}	Separation Factor	[-]
γ	Surface Tension	$[\frac{N}{m}]$
χ	TD – Tóth Constant	[-]
Abbreviations		
EWC	Expected Working Capacity	[mmol/g]
IAST	Ideal Adsorbed Solution Theory	

PSA	Pressure Swing Adsorption
SSR	Sum of Squares of Residual
TSA	Temperature Swing Adsorption
TPSA	Temperature Pressure Swing Adsorption
TVSA	Temperature Vacuum Swing Adsorption
VSA	Vacuum Swing Adsorption

APPENDIX

A. ECONOMIC ANALYSIS SAMPLE CALCULATIONS

A. ECONOMIC ANALYSIS SAMPLE CALCULATIONS

Figures 23 – 27 are examples of sample calculations performed for the economic analysis. This scenario represents the case if the process were to fully recover the ethylene adsorbed via the desorption process.

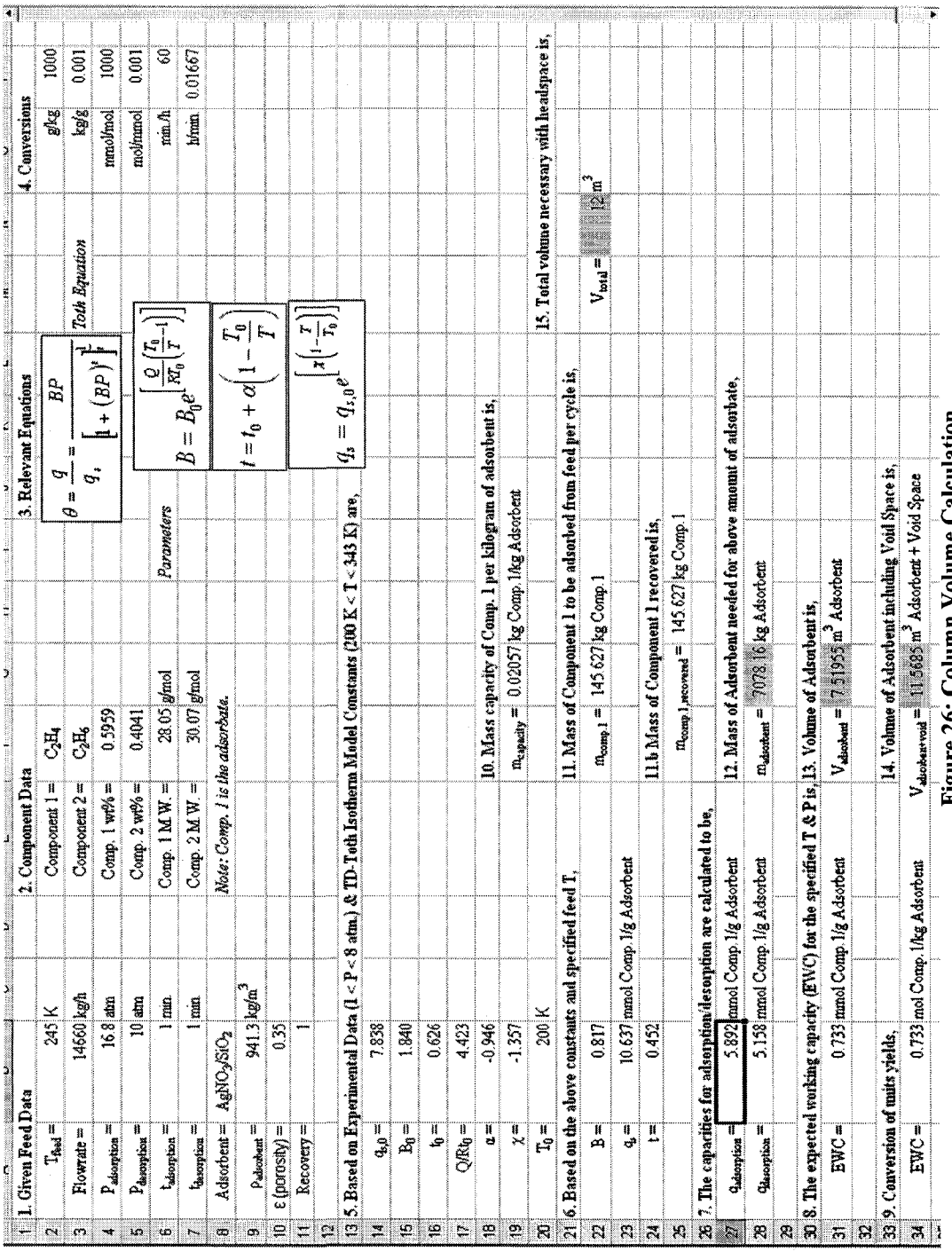

1. Given Feed Data

T_{feed} =	245	K
Flowrate =	14660	kg/h
$P_{adsorption}$ =	16.8	atm
$P_{desorption}$ =	10	atm
$t_{adsorption}$ =	1	min
$t_{desorption}$ =	1	min
Adsorbent =	$AgNO_3/SiO_2$	
$\rho_{adsorbent}$ =	941.3	kg/m^3
ε (porosity) =	0.35	
Recovery =	1	

2. Component Data

Component 1 =	C_2H_4		
Component 2 =	C_2H_6		
Comp. 1 wt% =	0.5959		
Comp. 2 wt% =	0.4041		
Comp. 1 M.W. =	28.05	g/mol	
Comp. 2 M.W. =	30.07	g/mol	
Note: Comp. 1 is the adsorbate.			

3. Relevant Equations

$$\theta = \frac{q}{q_s} = \frac{BP}{\left[1 + (BP)^t\right]^{\frac{1}{t}}}$$ *Toth Equation*

Parameters

$$B = B_0 e^{\left[\frac{Q}{RT_0}\left(\frac{T_0}{T}-1\right)\right]}$$

$$t = t_0 + \alpha\left(1 - \frac{T_0}{T}\right)$$

$$q_s = q_{s,0} e^{\left[\chi\left(1-\frac{T}{T_0}\right)\right]}$$

4. Conversions

g/kg	1000	
kg/g	0.001	
mmol/mol	1000	
mol/mmol	0.001	
min/h	60	
h/min	0.01667	

5. Based on Experimental Data (1 < P < 8 atm.) & TD-Toth Isotherm Model Constants (200 K < T < 343 K) are,

$q_{s,0}$ =	7.838
B_0 =	1.840
t_0 =	0.626
Q/Rt_0 =	4.423
α =	-0.946
χ =	-1.357
T_0 =	200 K

6. Based on the above constants and specified feed T,

B =	0.817	
q_s =	10.637	mmol Comp.1/g Adsorbent
t =	0.452	

7. The capacities for adsorption/desorption are calculated to be,

$q_{adsorption}$ =	5.892	mmol Comp.1/g Adsorbent
$q_{desorption}$ =	5.158	mmol Comp.1/g Adsorbent

8. The expected working capacity (EWC) for the specified T & P is,

EWC =	0.733	mmol Comp.1/g Adsorbent

9. Conversion of units yields,

EWC =	0.733	mol Comp.1/kg Adsorbent

10. Mass capacity of Comp. 1 per kilogram of adsorbent is,

$m_{capacity}$ = 0.02057 kg Comp.1/kg Adsorbent

11. Mass of Component 1 to be adsorbed from feed per cycle is,

$m_{comp.1}$ = 145.627 kg Comp.1

11.b Mass of Component 1 recovered is,

$m_{comp.1,recovered}$ = 145.627 kg Comp.1

12. Mass of Adsorbent needed for above amount of adsorbate,

$m_{adsorbent}$ = 7078.16 kg Adsorbent

13. Volume of Adsorbent is,

$V_{adsorbent}$ = 7.51995 m^3 Adsorbent

14. Volume of Adsorbent including Void Space is,

$V_{adsorbent+void}$ = 11.5685 m^3 Adsorbent + Void Space

15. Total volume necessary with headspace is,

V_{total} = 12 m^3

Figure 26: Column Volume Calculation

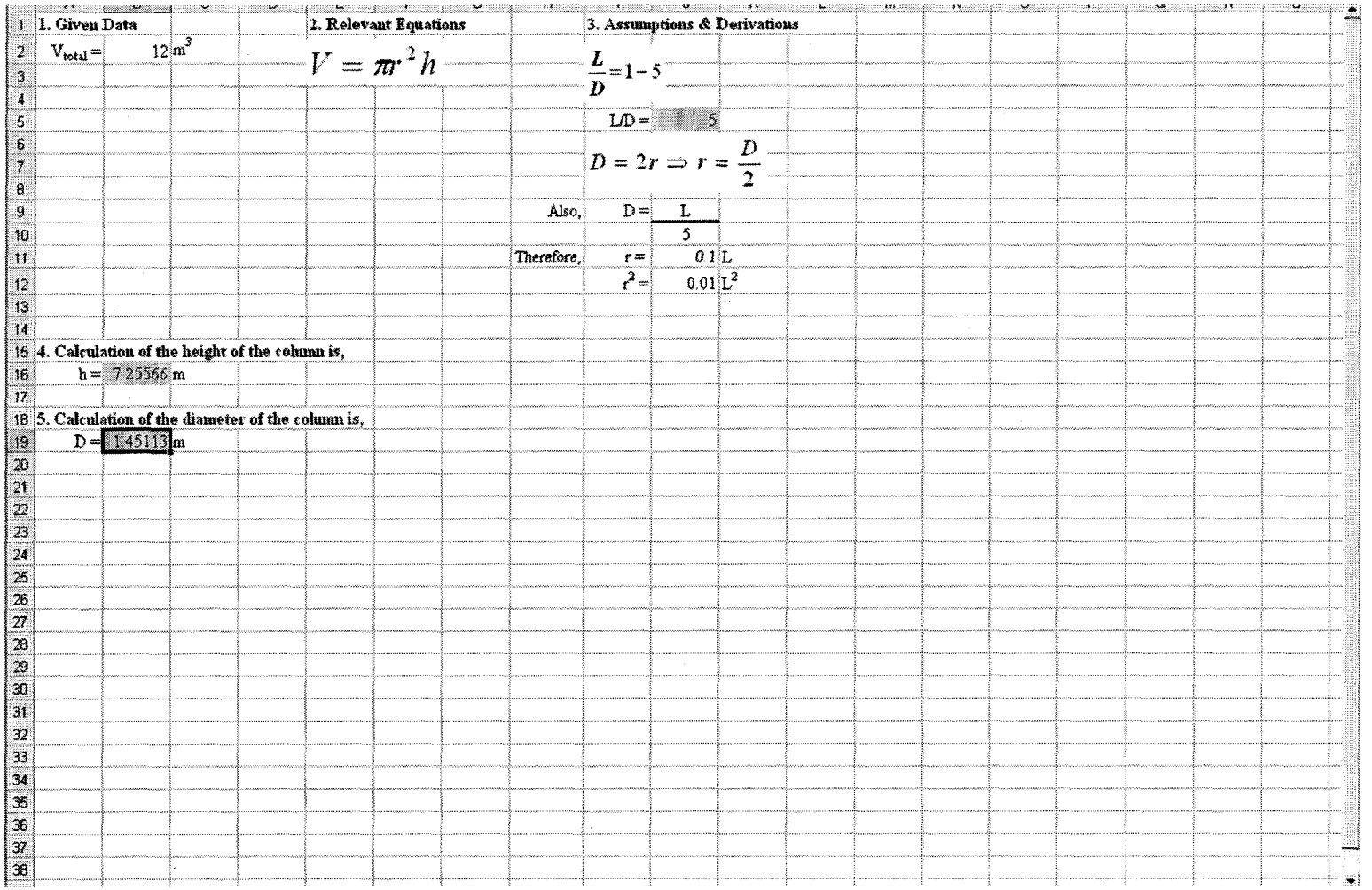

1. Given Data

V_{total} = 12 m^3

2. Relevant Equations

$$V = \pi r^2 h$$

3. Assumptions & Derivations

$$\frac{L}{D} = 1 - 5$$

L/D = 5

$$D = 2r \Rightarrow r = \frac{D}{2}$$

Also, $D = \frac{L}{5}$

Therefore, $r = 0.1\,L$

$r^2 = 0.01\,L^2$

4. Calculation of the height of the column is,

h = 7.25566 m

5. Calculation of the diameter of the column is,

D = 1.45113 m

Figure 27: Column Diameter & Height Calculation

Note: These equations come from Jules Thibault's Plant Design notes from 2005-2006.

Since we are using Impregnated Silica Gel, we use the following equation,

$$C_{P,Adsorbent} = 90\,S$$ (Seider et al., 2004)

Where $C_{P,Adsorbent}$ is the Purchase Cost of the Adsorbent [$]

S is the Size Factor [ft^3]

3. Calculation of Size Factor, S, is,

S = 265.5530212 ft^3

4. Calculation of Purchase Cost of Adsorbent is,

$C_{P,Adsorbent}$ = $23,899.77

Note: This value is valid for mid 1996, CEPCI = 382

5. Correcting cost for time using CEPCI method.

The following equation is used to update the values using CEPCI method.

$$C_2 = C_1 \frac{I_2}{I_1}$$ (Seider et al., 2004)

Where C_2 is the cost for present day (July, 2005)

C_1 is the cost for mid-1996

I_2 is the CEPCI index for present day (July, 2005) = 461.9

I_1 is the CEPCI index for mid-1996 = 382

C_2 = $28,898.70

This is a calculation of the most up to date quote provided from Sigma-Aldrich,

$29.00 per kg of SiO_2

$550 per kg of $AgNO_3$

m_{SiO2} = 5362.238958 kg

m_{AgNO3} = 1715.916467 kg

Therefore, the total cost for each individual component would be,

C_{SiO2} = $155,504.93

C_{AgNO3} = $943,754.06

Total = $1,099,258.99

2. Conversions

ft^3/m^3 35.315

Figure 28: Adsorbent Cost Calculation

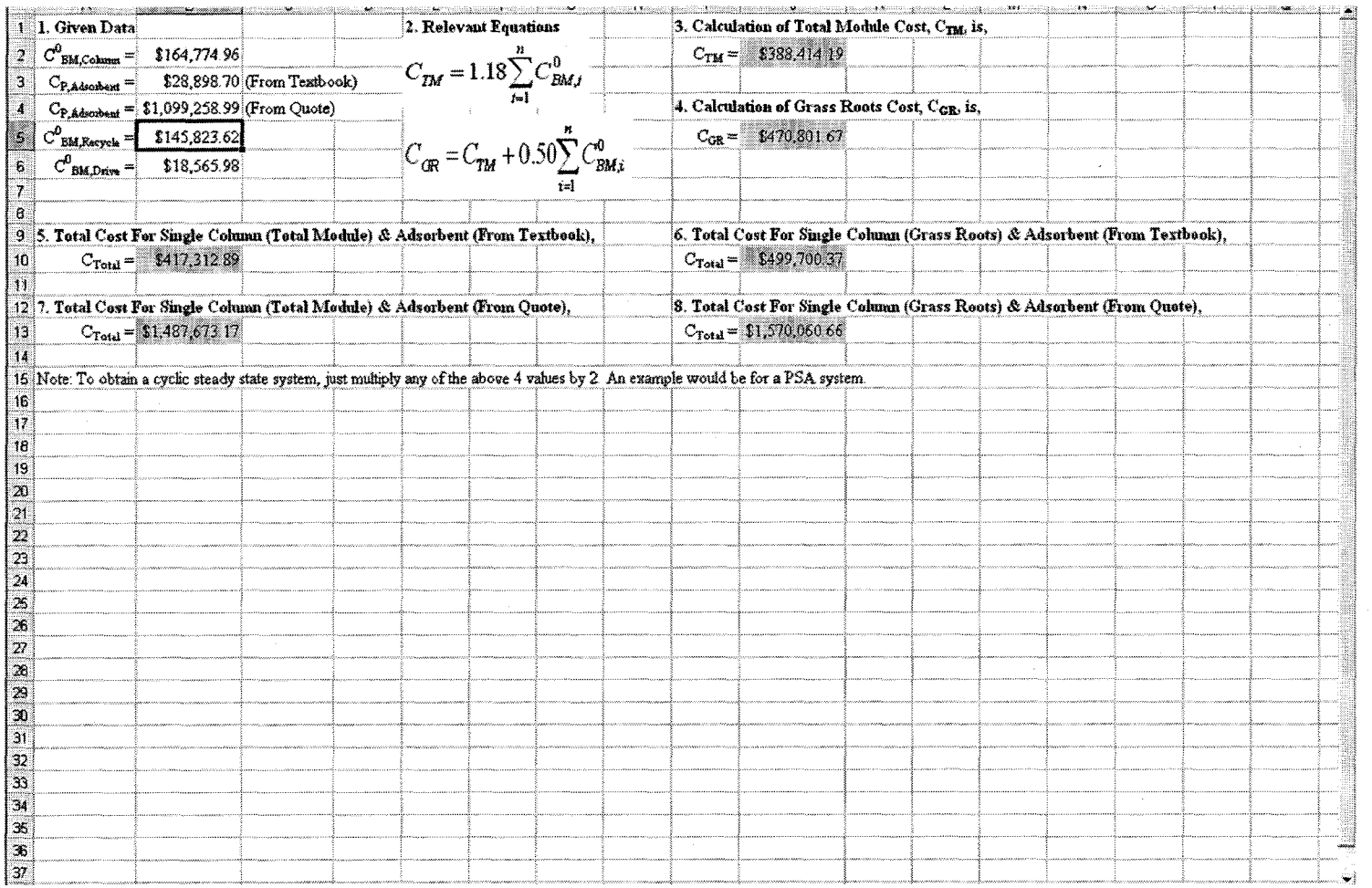

1	**1. Given Data**			**2. Relevant Equations**	**3. Calculation of Total Module Cost, C_{TM}, is,**
2	$C^0_{BM,Column}$ =	$164,774.96		$C_{TM} = 1.18\sum_{i=1}^{n} C^0_{BM,i}$	C_{TM} = $388,414.19
3	$C_{P,Adsorbent}$ =	$28,898.70	(From Textbook)		
4	$C_{P,Adsorbent}$ =	$1,099,258.99	(From Quote)		**4. Calculation of Grass Roots Cost, C_{GR}, is,**
5	$C^0_{BM,Recycle}$ =	$145,823.62		$C_{GR} = C_{TM} + 0.50\sum_{i=1}^{n} C^0_{BM,i}$	C_{GR} = $470,801.67
6	$C^0_{BM,Drive}$ =	$18,565.98			
7					
8					
9	**5. Total Cost For Single Column (Total Module) & Adsorbent (From Textbook),**				**6. Total Cost For Single Column (Grass Roots) & Adsorbent (From Textbook),**
10	C_{Total} =	$417,312.89			C_{Total} = $499,700.37
11					
12	**7. Total Cost For Single Column (Total Module) & Adsorbent (From Quote),**				**8. Total Cost For Single Column (Grass Roots) & Adsorbent (From Quote),**
13	C_{Total} =	$1,487,673.17			C_{Total} = $1,570,060.66
14					
15	Note: To obtain a cyclic steady state system, just multiply any of the above 4 values by 2. An example would be for a PSA system.				

Figure 29: Total Fixed Cost Calculation

1	**Summary for Fixed Cost**		
2	$m_{adsorbent}$	7078	kg Adsorbent
3	$V_{adsorbent}$	7.52	m^3 Adsorbent
4	$V_{adsorbent+void}$	11.57	m^3 Adsorbent + Void Space
5	V_{total}	12.00	m^3
6	Height	7.26	m
7	Diameter	1.45	m
8	$C_{P,Adsorbent}$	$28,898.70	**Method 1: Correlation calculated price of Silica Gel**
9	$C_{P,Adsorbent}$	$1,099,258.99	**Method 2: Quoted price of Silica Gel**
10	C^0_{BM}	$164,774.96	
11	C_{Total} =	$417,312.89	**Scenario 1: Correlation calculated price with addition to an existing distillation column**
12	C_{Total} =	$499,700.37	**Scenario 2: Correlation calculated price for an adsorption column alone**
13	C_{Total} =	$1,487,673.17	**Scenario 3: Quoted Adsorbent price with addition to an existing distillation column**
14	C_{Total} =	$1,570,060.66	**Scenario 4: Quoted Adsorbent price for an adsorption column alone**
15	$C_{Utility}$ =	$41,263.10	**Per Year**
16			
17			
18			
19			
20			
21			
22			
23			
24			
25			
26			
27			
28			
29			
30			
31			
32			
33			
34			
35			
36			
37			

Figure 30: Summary Table